Korean J Physiol Pharmacol 2017;21(5):531-546
https://doi.org/10.4196/kjpp.2017.21.5.531

KJPP

Original Article

Time-dependent proteomic and genomic alterations in Toll-like receptor-4-activated human chondrocytes: increased expression of lamin A/C and annexins

Seung Hee Ha[1,2,#], Hyoung Kyu Kim[1,#], Nguyen Thi Tuyet Anh[1], Nari Kim[1], Kyung Soo Ko[1], Byoung Doo Rhee[1], and Jin Han[1,*]

[1]National Research Laboratory for Mitochondrial Signaling, Department of Physiology, Department of Health Sciences and Technology, BK21 Plus Project Team, College of Medicine, Cardiovascular and Metabolic Disease Center, Inje University, Busan 47392, [2]Department of Health Technology Development, Health Project Management Team, Korea Health Industry Development Institute (KHIDI), Cheongju 28159, Korea

ARTICLE INFO

Received April 10, 2017
Revised May 4, 2017
Accepted May 10, 2017

***Correspondence**
Jin Han
E-mail: phyhanj@inje.ac.kr

Key Words
Annexin 4/5/6
Chondrocyte
Lamin A/C
Omics
Toll-like receptor-4

[#]These authors contributed equally to this study.

ABSTRACT Activation of Toll-like receptor-4 (TLR-4) in articular chondrocytes increases the catabolic compartment and leads to matrix degradation during the development of osteoarthritis. In this study, we determined the proteomic and genomic alterations in human chondrocytes during lipopolysaccharide (LPS)-induced inflammation to elucidate the underlying mechanisms and consequences of TLR-4 activation. Human chondrocytes were cultured with LPS for 12, 24, and 36 h to induce TLR-4 activation. The TLR-4-induced inflammatory response was confirmed by real-time PCR analysis of increased interleukin-1 beta (IL-1β), interleukin-6 (IL-6), and tumor necrosis factor alpha (TNF-α) expression levels. In TLR-4-activated chondrocytes, proteomic changes were determined by two-dimensional electrophoresis and matrix-assisted laser desorption/ionization-mass spectroscopy analysis, and genomic changes were determined by microarray and gene ontology analyses. Proteomics analysis identified 26 proteins with significantly altered expression levels; these proteins were related to the cytoskeleton and oxidative stress responses. Gene ontology analysis indicated that LPS treatment altered specific functional pathways including 'chemotaxis', 'hematopoietic organ development', 'positive regulation of cell proliferation', and 'regulation of cytokine biosynthetic process'. Nine of the 26 identified proteins displayed the same increased expression patterns in both proteomics and genomics analyses. Western blot analysis confirmed the LPS-induced increases in expression levels of lamin A/C and annexins 4/5/6. In conclusion, this study identified the time-dependent genomic, proteomic, and functional pathway alterations that occur in chondrocytes during LPS-induced TLR-4 activation. These results provide valuable new insights into the underlying mechanisms that control the development and progression of osteoarthritis.

INTRODUCTION

Articular cartilage contains a dense extracellular matrix (ECM) with highly specialized cells called chondrocytes [1]. The cartilage has a load-bearing function and provides mechanical stability to bones [2]. It contains a few chondrocytes with varying sizes and shapes according to the cartilage layer [1]. Chondrocytes modulate cartilage homeostasis by interacting

Author contributions: S.H.H. and H.K.K. designed experiments and performed proteomics and genomics experiments. N.T.T.A. and N.K. contributed to systemic analysis of proteome data. K.S.K. and B.D.R. contributed to the advice and supervision of the clinical significance of chondrocyte inflammation. J.H. supervised and coordinated the study. S.H.H. and H.K.K. wrote the manuscript.

with the extracellular environment that surrounds the matrix [2]. Degradation of the cartilage ECM is a major cause of articular destruction, which develops into rheumatoid arthritis, osteoarthritis, or septic arthritis. Chondrocytes respond to stimuli such as proinflammatory cytokines and mechanical load via cartilage-degrading enzymes and catabolic mediators [2,3]. Cartilage degradation is associated with increased expression of immunity mediators such as nitrogen oxide, interleukin-1 beta (IL-1β), and tumor necrosis factor alpha (TNF-α) [4]. The proinflammatory cytokines IL-1β and TNF-α are involved in the immune response in arthritis and cartilage degradation [2]. Inhibition of IL-1β and TNF-α signaling effectively reduces inflammation, cartilage degradation, and arthritis, although inhibiting the individual signaling pathways rarely protects the joint. There is a lack of studies on other signaling pathways mediating catabolism in the joint [5,6]. Several studies report that oncostatin M, fibronectin fragments, and retinoic acid induce chondrocyte-mediated catabolism, thereby reducing the aggrecan proteoglycan levels in cartilage [7-9].

Toll-like receptors (TLRs) have crucial functions in inflammatory diseases [10-12] because they recognize pathogen-associated molecular patterns (PAMPs) and serve as the first line of defense against pathogen invasion [13,14]. TLRs are major sensors of viral products and are expressed in dendritic cells and macrophages, both of which are sentinels of the immune system [13,15]. A total of 13 TLRs have been identified in humans; TLR 1, 2, 4, 5, 6, and 11 are localized on the cell surface, whereas TLR 3, 7, 8, and 9 are localized inside the cell [16]. Human articular chondrocytes express several TLRs, including TLR-2 and TLR-4 [17]. All human TLRs are adaptor proteins, excluding MyD88 and TLR-3 [16]. TLR activation in chondrocytes increases the catabolic compartment, which induces matrix degradation [18]. TLR-2 and TLR-4 expression increases in the articular cartilage of people with osteoarthritis, and inflammatory mediators such as IL-1β and TNF-α induce increased expression of TLR-2 and TLR-4 in cultured chondrocytes [19].

Lipopolysaccharide (LPS) is a complex molecule containing a lipid moiety and a polysaccharide. LPS is an important constituent of Gram-negative bacteria and activates the congenital immune system [10]. LPS is used to induce cartilage matrix degradation and stimulate pyrogenic arthritis in *in vitro* experiments, and to stimulate cytokine production in chondrocytes [20]. In articular chondrocytes, LPS inhibits cellular proliferation and proteoglycan synthesis in a concentration-dependent manner, and stimulates proteoglycan degradation [20,21]. TLR activation in articular chondrocytes increases matrix metalloproteinases (MMPs) [22]. A recent study suggested that TLRs mediate LPS signaling in target cells [23]. Although TLR-2 was reported to be involved in LPS signaling [24], the most essential receptor for LPS signaling is TLR-4 [25]. In arthritis mediated by the immune complex, TLR-4 modulates the early onset of immunity and cartilage destruction by increasing cytokine production and IL-10-mediated expression of Fc-gamma receptors [26]. $TLR4^{-/-}$ mice did not display LPS-induced chondrocyte activation and procatabolic response [14]. A previous proteomic study reported that TLR4-mediated activation of rat chondrocytes induced innate immune responses, which increased the production of long pentraxin-3, chitinase-3-like protein1, and osteoglycin [22]. However, TLR-4-mediated activation of time-dependent proteomic and genomic alterations in human chondrocytes has not been fully elucidated. In this study, both proteomic and genomic analyses were performed to elucidate the signaling mechanisms involved in TLR-4 activation in a human chondrocyte cell line.

METHODS

Chondrocyte cultures

Human chondrocyte cells CHON002, derived from a female patient (American Type Culture Collection, Manassas, VA, USA), were cultured in 100 mm dishes containing 10 ml of Dulbecco's modified Eagle's medium (DMEM; American Type Culture Collection, Manassas, VA, USA) supplemented with 10% fetal bovine serum (FBS; Premium Fetal Bovine Serum, Lonza, Basel, Switzerland) and 0.1 mg/ml G-418 sulfate (cell culture tested, Calbiochem, San Diego, USA). Cultures were incubated at 37°C in humidified air with 5% CO_2. When the chondrocyte cultures reached 80% confluence, the cells were washed with phosphate-buffered saline (PBS; Dulbecco's Phosphate-Buffered Saline, Invitrogen, Carlsbad, USA), treated with a Trypsin-Versene (EDTA) mixture (Lonza), and subcultured. The medium was routinely changed every 2 days. At passage 6, chondrocytes were cultured at 37°C for 24 h in DMEM containing 1% FBS and 0.1 mg/ml G-418 sulfate, and stabilized. After a 24 h culture, chondrocytes were washed three times in PBS, and collected by centrifugation (1,000×*g*, 3 min) after each wash.

TLR-4 activation

The lipopolysaccharide (LPS) (L4391, Sigma, St. Louis, MO) was used for activation of TLR-4 in cultured chondrocytes. Twenty-four hours stabilized chondrocytes were treated with 1 μg/ml LPS and incubated for 12, 24, or 36 h. After each incubation period, the treated chondrocytes were harvested in the same way as the non-treated control group.

Two-dimensional gel electrophoresis and proteomics analysis

Proteomic analysis of chondrocytes was performed by two-dimensional gel electrophoresis (2DE) and matrix-assisted laser desorption/ionization-time of flight mass spectrometry (MALDI-TOF MS) analysis as described previously [27] (detailed

methods are provided in the online Supplementary Materials). Protein expression levels were quantified using the digitized gel image analyzer PDQuest version 7.0 (Bio-Rad, Hercules, CA). Proteins that displayed >2-fold increases or decreases after LPS treatment ($p<0.05$), compared with matched control proteins, were selected for further analysis and identification. The search program MASCOT (http://www.matrixscience.com/cgi/ search_form.pl?FORMVER=2&SEARCH=PMF) was used for protein identification by peptide mass fingerprinting. Spectra were calibrated with trypsin auto-digestion ion peak m/z (842.510, 2211.1046) as internal standards. The quality of protein identification was evaluated by Molecular Weight Search (MOWSE) score [28].

Microarray and genomics analysis

Genomic analysis of chondrocytes was performed using the Agilent Whole Human Genome Oligo Microarray (44K) as described previously (Agilent Technology, Santa Clara, CA, USA) [29] (detailed methods are provided in the online Supplementary Materials). The hybridized microarrays were scanned using the Agilent DNA Microarray Scanner, and then were quantified with Feature Extraction Software (Agilent Technology). All data normalization and selection of fold-changed genes were performed with GeneSpringGX v. 7.3 (Agilent Technology). The normalized ratio averages were calculated by dividing the average of normalized test channel intensity by the average of normalized control channel intensity. Functional annotation of genes was performed according to the Gene Ontology Consortium (http://www.geneontology.org/index.shtml) using GeneSpringGX v. 7.3 [29,30].

Real-time PCR analysis

For real-time PCR analysis, 2 μg of total RNA were reverse-transcribed using TaqMan Reverse Transcription Reagent (ABI, Foster City, CA). Before reverse transcription, each sample of total RNAs was treated with 10U of DNase I. Each cDNA sample was additionally prepared in the absence of enzyme and used as a negative control to estimate the amount of contaminating DNA. From the final 20 μl reaction mix, 1 μl was used as a template in duplicate PCR reactions in a Prism 7900HT Sequence Detection System (ABI, Foster City, CA). Cycling conditions were as follows: 2 min at 50°C; 5 min at 95°C; and 35 cycles of 15 s at 95°C, 15 s at 55°C, and 20 s at 72°C. The *GAPDH* gene was used as a standard for each plate. The primers for each gene examined in our study are listed in Table 1. The relative quantity of each gene was calculated using data from standard curves, and all data were normalized with respect to that of *GAPDH*.

Western blot analysis

The collected chondrocyte cells were sonicated in 1% NP-40 lysis buffer [150 mM NaCl, 20 mM Tris-HCl (pH 7.5), 1% glycerol, 1% Nonidet-P40, and 10% protease inhibitor] 10 times for 3 s each using a Sonoplus sonicator (Bandelin Electronic, Germany). The sonicated samples were centrifuged (16,000×*g*, 4°C, 30 min), and the supernatant was transferred to a new Eppendorf tube. Protein concentrations were measured using the 2-D Quant Kit (Amersham Biosciences, Little Chalfont, UK). Then, 15 μg of proteins were mixed with 1% NP-40 and 5× sample buffer and denatured at 98°C for 5 min. The denatured proteins were loaded on a 7.5% SDS-polyacrylamide gel and separated by electrophoresis at 80 V for 30 min and 110 V for 90 min. Protein sizes were confirmed by comparison with the DokDo-MARK protein marker (EBM-1032, Elpis-Biotech, Daejeon, Korea). Separated proteins were transferred from the gel to a nitrocellulose membrane (Hybond-ECL, Amersham Biosciences, Little Chalfont, UK) at 25 V for 45 min. The membrane was blocked overnight in 5% non-fat milk at room temperature and then washed three times with TBS-T [10 mM Tris (pH 7.6), 3 mM NaCl, and 0.5% Tween 20] for 15 min. The blocked membrane was probed with antibodies to lamin A/C (Cell Signaling Technology, Beverly, MA, USA) or annexin 4/5/6 (Abcam, Cambridge, MA, USA), at 4°C overnight, and then washed three times with TBS-T for 15 min. The membrane was incubated with HRP-conjugated Rabbit IgG (1:10,000 dilution, EnZo Life Sciences, Plymouth Meeting, PA, USA) at room temperature for 1 h, and then washed three times with TBS-T for 15 min. The resulting bands were visualized with SuperSignal West Pico Chemiluminescent Substrate (Thermo Fisher Scientific, Waltham, MA, USA) using the Las-3000 image reader (Fuji Film, Miyagi, Japan)[31].

Gene ontology analysis and functional annotation of proteins

We categorized and annotated identified proteins and genes using the Swiss-Prot and PANTHER (protein analysis through evolutionary relationships) databases to understand their molecular functions and biological processes. Protein-protein

Table 1. Primers used for real-time PCR

Gene	Size (bp)		Sequence (5' → 3')
TNF-α	92	Forward	CCTCCACCCATGTGCTCCTC
		Reverse	GGGGCTCTTGATGGCAGAGA
IL-6	111	Forward	CAAGCCAGAGCTGTGCAGATG
		Reverse	CAGGCTGGCATTTGTGGTTG
IL-1β	120	Forward	TGGAAAAGCGATTTGTCTTCAACA
		Reverse	CCAGGAAGACGGGCATGTTT

interactions between identified proteins and constructed protein networks were analyzed using the online STRING 8.3 database and Cytoscape software version 2.6.3. Gene ontology (GO) and functional enrichment analyses were performed using DAVID bioinformatics resources (https://david.ncifcrf.gov/) [32].

Statistical analysis

All results are expressed as the mean±SEM, which were calculated using Origin 6.0 software (Microcal Software, Northampton, MA). Student's *t*-test was used to compare values between groups, and $p<0.05$ was considered to indicate statistical significance.

RESULTS

Changes in chondrocyte morphology during TLR-4 activation

To examine the effect of TLR-4 activation on the external shape of chondrocytes, chondrocytes were treated with 1 μg/ml LPS for 12, 24, and 36 h. Treated cells were viewed under a microscope (×200). The cellular shapes of chondrocytes in control and experimental groups did not significantly differ (Fig. 1A).

Changes in cytokine expression in LPS-treated chondrocytes

Changes in cytokine expression in LPS-treated chondrocytes were investigated using real-time PCR analysis. The results indicated that the expression levels of TNF-α, IL-1β, and IL-6 were higher in the LPS-treated group than in the control group (Fig. 1B). The TNF-α level increased 15.65-fold after 36 h of LPS treatment compared with that of the control. The expression of IL-1β and IL-6 peaked after 12 h, and then slightly decreased over time. These results indicate that activation of the LPS ligand TLR-4 in chondrocytes led to increased expression of the inflammatory mediators TNF-α, IL-1β, and IL-6, which was followed by increased expression of TLR-4 and the consequent inflammatory response.

Proteomic profiling of LPS-activated chondrocytes

TLR-4 was activated by treating the chondrocytes with LPS for 12, 24, and 36 h. Then, 2DE was performed to examine changes in protein expression (Fig. 2A). The protein spots were separated using a pH gradient that ranged from 4 to 10 and a molecular weight (MW) gradient that ranged from 10 to 200 kDa. A total of 900 protein spots were observed (Supplementary Fig. 1). Of these, 27 protein spots (3%) displayed ≥1.5-times changes in expression levels at 12, 24, and 36 h. Of these 27 protein spots, seven changed after LPS treatment for 12 h (five increased and two decreased), 17 changed after 24 h treatment (17 increased), and 24 changed after 36 h treatment (24 increased) (Fig. 2B). These spots were cut from the gel and digested with trypsin. Then, the digested proteins were analyzed by performing MALDI-TOF MS. Of the 27 protein spots, A total of 26 proteins were identified using MS/MS data according to the degree of activated TLR-mediated expression and the time of LPS treatment (Table 2). We listed the protein information including, protein name, SWISS Prot ID, protein molecular weight (MW) and isoelectric point (pI), MOWSE score, and relative protein expression level of LPS treated chondrocyte/control chondrocyte group at different time points (12 h, 24 h and 36 h) in the Table 2. Changes in the protein expression levels were examined according to the protein identification results. Lamin A/C expression increased ≥1.5 times when chondrocytes were treated with LPS for 24 or 36 h. SOD-2 expression increased ≥2 times at 12 h of LPS treatment. Cofilin and Caldesmon expression decreased ≥1.5 times at 12 h of LPS treatment, but increased at 24 and 36 h (Fig. 2C).

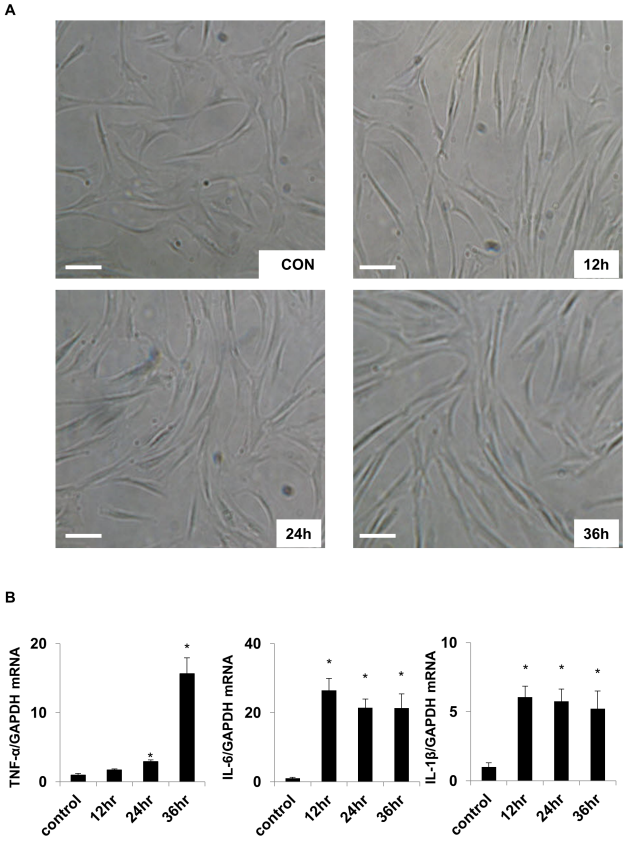

Fig. 1. LPS-induced changes in chondrocyte morphology and cytokine expression. (A) Morphology of cultured human chondrocytes. Images of untreated control (CON), and after LPS treatment for 12, 24, and 36 h to activate TLR-4 (×200 magnification). Scale bar=100 μm. (B) Relative changes in mRNA expression of selected cytokines including TNF-α, IL-6, and IL-1β. Internal standard was GAPDH.

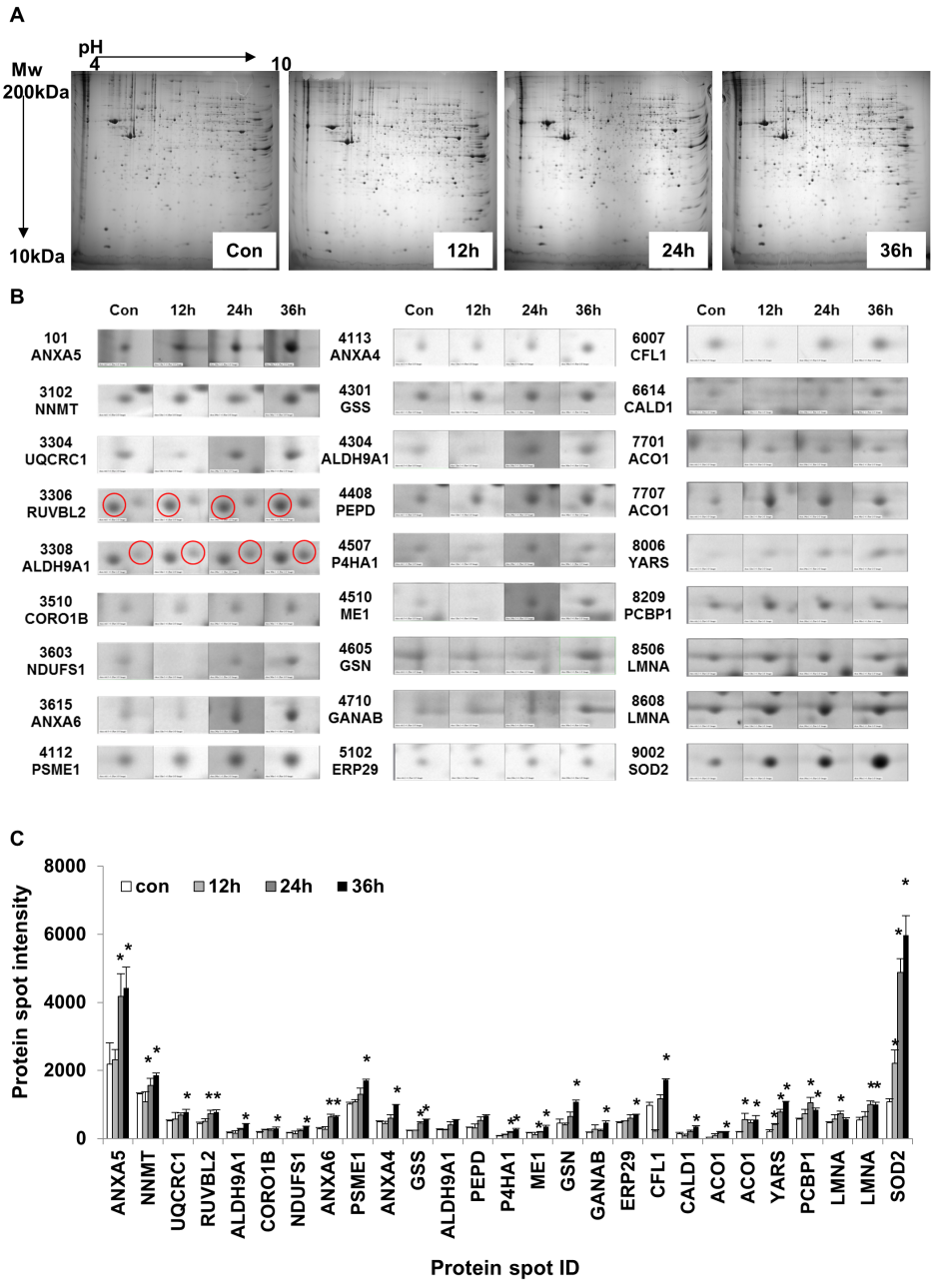

Fig. 2. Two-dimensional gel electrophoresis patterns of proteins in control and LPS-treated chondrocytes. (A) Proteins (200 μg each) isolated from of untreated control (Con) chondrocytes and after LPS treatment for 12, 24, and 36 h to activate TLR-4. Proteins were separated in the 20×24 cm gel with pH ranging from 4 to 10. (B) Twenty-seven significantly changed protein spots were selected for MALDI-TOF MS analysis to identify proteins (C). Histogram of time-dependent protein expression levels in untreated control (CON) chondrocytes and after LPS treatment for 12, 24, and 36 h to activate TLR-4 (*p<0.05).

Annotation of identified proteins and systemic analysis

Several types of systemic analyses were used to identify the molecular functionality and biological process of the identified proteins and interactions between the proteins. First, detailed information on the identified proteins was obtained using the STRING 8.0 database (Table 3), and the degree of expression change was examined by process and function using the PANTHER Classification System (Supplementary Fig. 2 and Table 4). Table 4 shows the biological process and molecular function of each identified proteins. Briefly, activation of TLR-4 in chondrocytes changed the molecular functions in the following order: catalytic activity (47%), binding (33%), structural molecule activity (13%), and transcription regulator activity (7%) (Supplementary Fig. 2A). The biological processes of metabolic process (32%), cellular process (15%), and transport (9%) were most affected by TLR-4 activation in PANTHER classification algorithm (Supplementary Fig. 2B).

Table 4 shows the identified protein functions based on the Swiss-Prot database. Lamin A/C is a structural constituent of the cytoskeleton. The protein-protein interactions (PPI) of the identified proteins were analyzed as follows. First, the network map of the identified proteins was investigated using the STRING 8.3 analysis program (Fig. 3A). The network consisted of 24 proteins and 12 interactions, and the 12 interactions

Table 2. MALDI-TOF identification of significantly altered protein expression in TLR-4-activated chondrocytes

Sample	Protein name	Swiss-Prot	MW/pI[1]	Score[2]	12 h LPS/con	24 h LPS/con	36 h LPS/con
101	Annexin A5	P08758	75826/5.42	109	1.29	2.14	2.26
3102	Nicotinamide N-methyltransferase	P40261	29555/5.56	61	0.82	1.18	1.41
3304	Cytochrome b-c1 complex subunit1, mitochondrial	P31930	52612/5.94	48	1.11	1.32	1.50
3306	RuvB-like 2	Q9Y230	51125/5.49	232	1.16	1.63	1.77
3308	4-trimethylaminobutyraldehyde dehydrogenase	P49189	53767/5.69	119	1.02	1.64	2.56
3510	Coronin-1B	Q9BR76	54200/5.61	49	1.39	1.35	1.66
3603	NADH-ubiquinone oxidoreductase 75 kDa subunit, mitochondrial	P28331	79417/5.89	31	0.81	1.43	2.25
3615	Annexin A6	P08133	75826/5.42	109	0.96	2.38	2.49
4112	Proteasome activator subunit 1 isoform 1	NP_006254	28705/5.78	246	1.06	1.27	1.68
4113	Annexin A4	P09525	35860/5.84	127	0.92	1.24	2.03
4301	Glutathione synthetase	P48637	52352/5.67	109	1.05	1.99	2.47
4304	4-trimethylaminobutyraldehyde dehydrogenase	P49189	53767/5.69	34	0.97	1.58	2.10
4408	Xaa-Pro dipeptidase	P12955	54513/5.64	99	0.94	1.63	2.11
4507	Prolyl 4-hydroxylase subunit alpha-1	P13674	61011/5.70	36	1.36	2.23	3.35
4510	NADP-dependent malic enzyme	P48163	64109/5.79	79	0.67	1.15	2.03
4605	Gelsolin	P06396	85644/5.90	72	0.99	1.61	2.84
4710	Neutral alpha-glucosidase AB	Q14697	106807/5.74	58	1.54	1.37	2.71
5102	Endoplasmic reticulum protein ERp29	P30040	28975/6.77	107	1.10	1.28	1.51
6007	Cofilin-1	P23528	18491/8.22	110	0.24	1.24	1.80
6614	Caldesmon	Q05682	93194/5.63	53	0.45	1.93	3.35
7701	Cytoplasmic aconitate hydratase	P21399	98337/6.23	32	2.51	4.80	5.29
7707	Cytoplasmic aconitate hydratase	P21399	98337/6.23	46	3.23	2.61	2.91
8006	Tyrosine--tRNA ligase, cytoplasmic	P54577	59106/6.61	47	2.17	4.42	5.79
8209	Poly (rC)-binding protein 1	Q15365	37474/6.66	49	1.24	1.85	1.46
8506	Lamin isoform A	NP_733821	74095/6.57	120	1.30	1.61	1.26
8608	Lamin A protein	AAA36160	74095/6.57	49	1.32	1.96	1.94
9002	Superoxide dismutase [Mn], mitochondrial	P04179	24707/8.35	67	2.10	4.71	5.72

[1]pI (isoelectric point) and protein MW were obtained from the MASCOT database. [2]Score, MOWSE score: Molecular Weight Search score [28].

involved 14 (58.3%) of the total of 24 proteins. Upregulation or downregulation of protein expression was marked in the network map, and showed dynamic alterations in protein expression levels during LPS-induced inflammation in chondrocytes. The largest number of proteins changed expression after LPS treatment for 36 h. Then, the 36 h and 12 h treatment groups were compared and visualized on the network map using Cytoscape to identify changes in expression levels according to the LPS treatment time (Figs. 3B-D). When chondrocytes were treated with LPS for 12 h, the levels of NNMT, NDUFS1, ANXA6, ANXA4, ALDH9A1, PEPD, ME1, GSN, CFL1, and CALD1 decreased (Fig. 3B). When chondrocytes were treated with LPS for 24 and 36 h, the expression of all proteins clearly increased (Figs. 3C and D). When lamin A/C was viewed as the center of the network map, it formed a directly connected network with YARS and PCBP1. This network also included ACO1, ALDH9A1, SOD2, GSS, NDUFS1, and UQCRC1, which are involved in mitochondrial energy metabolism and antioxidant regulating proteins.

Genomic profiling of LPS-activated chondrocytes

Total RNA was extracted from LPS-treated chondrocytes using the same conditions that were used for 2DE proteomic analysis. Then, cDNA was synthesized and changes in genomic expression profiles were analyzed using the Agilent Human Whole-Genome 44K DNA Chip Microarray (Supplementary Fig. 3). We compared the degree of gene expression of the LPS-treated groups that were classified according to their LPS treatment time for the activation of TLR-4 with that in the control group. A significance test was performed using a scatter plot. In the supplementary Fig. 3A, the red dots over the slope that is close to the longitudinal axis represent the genes that were found to have increased two fold or more when each LPS-treated group and the control group were compared, and the green dots under the slope that is close to the horizontal line represent the genes that were found to have decreased two fold or more when each of the LPS-treated groups and the control group were compared. A total of 2,929 genes increased more than two fold, and 2,839 genes decreased more than two fold in all groups. The degree of expression of the genes

Table 3. Functional annotation of identified proteins

Spot no.	Swiss-Prot	Symbol	Description
101	P08758	ANXA5	Annexin A5 is an anticoagulant protein that acts as an indirect inhibitor of the thromboplastin-specific complex.
3102	P40261	NNMT	Catalyzes the N-methylation of nicotinamide and other pyridines to form pyridinium ions; this activity is important for biotransformation of many drugs and xenobiotic compounds.
3304	P31930	UQCRC1	Ubiquinol-cytochrome-c reductase complex core protein 1, mitochondrial precursor, is a component of the ubiquinol-cytochrome c reductase complex (complex III or cytochrome b-c1 complex), which is part of the mitochondrial respiratory chain; this protein may mediate formation of the complex between cytochromes c and c1.
3306	Q9Y230	RUVBL2	RuvB-like 2 (48 kDa TATA box-binding protein-interacting protein); Possesses single-stranded DNA-stimulated ATPase and ATP- dependent DNA helicase (5' to 3') activity; component of the NuA4 histone acetyltransferase complex which is involved in transcriptional activation of select genes principally by acetylation of nucleosomal histone H4 and H2A.
3308, 4304	P49189	ALDH9A1	4-trimethylaminobutyraldehyde dehydrogenase (Aldehyde dehydrogenase 9A1); converts gamma-trimethylaminobutyraldehyde into gamma-butyrobetaine; catalyzes the irreversible oxidation of a broad range of aldehydes to the corresponding acids in an NAD-dependent reaction.
3510	Q9BR76	CORO1B	Coronin-1B (Coronin-2); regulates leading edge dynamics and cell motility in fibroblasts; may be involved in cytokinesis and signal transduction (by similarity).
3603	P28331	NDUFS1	NADH-ubiquinone oxidoreductase 75 kDa subunit, mitochondrial precursor; core subunit of the mitochondrial membrane respiratory chain NADH dehydrogenase (Complex I) that is believed to belong to the minimal assembly required for catalysis; complex I functions in the transfer of electrons from NADH to the respiratory chain; the immediate electron acceptor for the enzyme is believed to be ubiquinone (by similarity); this is the largest subunit of complex I and is a component of the iron-sulfur (IP) fragment of the enzyme.
3615	P08133	ANXA6	Annexin A6 (Annexin VI, Lipocortin VI) may associate with CD21; may regulate the release of Ca^{2+} from intracellular stores.
4112	NP_006254	PSME1	Proteasome activator complex subunit 1 (Activator of multicatalytic protease subunit 1); implicated in immunoproteasome assembly and is required for efficient antigen processing; the PA28 activator complex enhances the generation of class I binding peptides by altering the cleavage pattern of the proteasome.
4113	P09525	ANXA4	Annexin A4 (Annexin IV, Lipocortin IV); Calcium/phospholipid-binding protein that promotes membrane fusion and is involved in exocytosis (by similarity).
4301	P48637	GSS	Glutathionesynthetase
4408	P12955	PEPD	Xaa-Pro dipeptidase (X-Pro dipeptidase); splits dipeptides with a prolyl or hydroxyprolyl residue in the C-terminal position; plays an important role in collagen metabolism because of the high level of iminoacids in collagen.
4507	P13674	P4HA1	Prolyl 4-hydroxylase subunit alpha-1 precursor (4-PH alpha-1); catalyzes the posttranslational formation of 4- hydroxyproline in -Xaa-Pro-Gly- sequences in collagens and other proteins.
4510	P48163	ME1	NADP-dependent malic enzyme (NADP-ME)
4605	P06396	GSN	Gelsolin precursor (Actin-depolymerizing factor); calcium-regulated, actin-modulating protein that binds to the plus (or barbed) ends of actin monomers or filaments, preventing monomer exchange (end-blocking or capping); it can promote the assembly of monomers into filaments (nucleation) as well as sever filaments already formed.
4710	Q14697	GANAB	Neutral alpha-glucosidase AB precursor (Glucosidase II subunit alpha); sequentially cleaves the two innermost alpha-1,3-linked glucose residues from the Glc(2)Man(9)GlcNAc(2) oligosaccharide precursor of immature glycoproteins.
5102	P30040	ERP29	Endoplasmic reticulum protein ERp29 precursor; does not seem to be a disulfide isomerase; plays an important role in the processing of secretory proteins within the endoplasmic reticulum (ER), possibly by participating in the folding of proteins in the ER.
6007	P23528	CFL1	Cofilin-1 (Cofilin, nonmuscle isoform); reversibly controls actin polymerization and depolymerization in a pH-sensitive manner; it has the ability to bind G- and F-actin at a 1:1 ratio of cofilin to actin; it is the major component of intranuclear and cytoplasmic actin rods.
6614	Q05682	CALD1	Caldesmon (CDM); Actin- and myosin-binding protein implicated in the regulation of actomyosin interactions in smooth muscle and nonmuscle cells (could act as a bridge between myosin and actin filaments); stimulates actin binding of tropomyosin, which increases the stabilization of actin filament structure; in muscle tissues, it inhibits the actomyosin ATPase by binding to F-actin; this inhibition is attenuated by calcium-calmodulin and is potentiated by tropomyosin; interacts with actin, myosin, two molecules of tropomyosin, and with calmodulin.

Table 3. Continued

Spot no.	Swiss-Prot	Symbol	Description
7701, 7707	P21399	ACO1	Iron-responsive element-binding protein 1 (IRE-BP 1); binds to iron-responsive elements (IRES), which are stem-loop structures found in the 5'-UTR of ferritin and delta aminolevulinic acid synthase mRNAs, and in the 3'-UTR of transferrin receptor mRNA; binding to the IRE element in ferritin results in the repression of its mRNA translation.
8006	P54577	YARS	Tyrosyl-tRNA synthetase, cytoplasmic (Tyrosyl--tRNA ligase); catalyzes the attachment of tyrosine to tRNA (Tyr) in a two-step reaction: tyrosine is first activated by ATP to form Tyr-AMP and then transferred to the acceptor end of tRNA (Tyr) (by similarity).
8209	Q15365	PCBP1	Poly (rC)-binding protein 1 (Alpha-CP1); single-stranded nucleic acid binding protein that binds preferentially to oligo dC.
8506, 8608	NP_733821	LMNA	Lamin A/C (70 kDa Lamin) (Renal carcinoma antigen NY-REN-32); Lamins are components of the nuclear lamina, a fibrous layer on the nucleoplasmic side of the inner nuclear membrane, which is thought to provide a framework for the nuclear envelope and may also interact with chromatin; Lamins A and C are present in equal amounts in the lamina of mammals.
9002	P04179	SOD2	Superoxide dismutase [Mn], mitochondrial precursor; destroys radicals which are normally produced within the cells and which are toxic to biological systems (by similarity).

Table 4. Molecular functions and biological processes of identified proteins

NCBI access	Protein name	Symbol	Biological process	Molecular function
P49189	4-trimethylaminobutyraldehydede-hydrogenase	ALDH9A1	Carbohydrate metabolic process	Oxidoreductase activity
Q14697	Neutral alpha-glucosidase AB	GANAB		Hydrolase activity, hydrolyzing O-glycosyl compounds
P23528	Cofilin-1	CFL1	Cellular component morphogenesis	Structural constituent of cytoskeleton
Q05682	Caldesmon	CALD1		Structural constituent of cytoskeleton
P06396	Gelsolin	GSN		Structural constituent of cytoskeleton
NP_733821	Lamin isoform A	LMNA		Structural constituent of cytoskeleton
Q9BR76	Coronin-1B	CORO1B	Intracellular protein transport	Structural constituent of cytoskeleton
P30040	Endoplasmic reticulum protein ERp29	ERP29		Exocytosis
P40261	Nicotinamide N-methyltransferase	NNMT	Metabolic process	Methyltransferase activity
Q9Y230	RuvB-like 2	RUVBL2	Nucleobase, nucleoside, nucleotide and nucleic acid metabolic process	DNA helicase activity
Q15365	Poly(rC)-binding protein 1	PCBP1		RNA splicing factor activity
P13674	Prolyl 4-hydroxylase subunit alpha-1	P4HA1	Oxygen and reactive oxygen species metabolic process	Oxidoreductase activity
P04179	Superoxide dismutase [Mn], mitochondrial	SOD2		Oxidoreductase activity antioxidant
NP_006254	Proteasome activator subunit 1 isoform 1	PSME1	Protein metabolic process	Protease
P12955	Xaa-Pro dipeptidase	PEPD		Peptidase activity
P54577	Tyrosyl-tRNA synthetase, cytoplasmic	YARS		Aminoacyl-tRNA ligase activity
P31930	Cytochrome b-c1 complex subunit1, mitochondrial	UQCRC1	Respiratory electron transport chain	Oxidoreductase activity
P28331	NADH-ubiquinone oxidoreductase 75 kDa subunit, mitochondrial	NDUFS1		Oxidoreductase activity
P08758	Annexin A5	ANXA5	Signal transduction	Calcium-dependent phospholipid-binding
P08133	Annexin A6	ANXA6		Calcium-dependent phospholipid-binding
P09525	Annexin A4	ANXA4		Calcium-dependent phospholipid-binding
P48637	Glutathionesynthetase	GSS	Sulfur metabolic process	Ligase activity antioxidant
P48163	NADP-dependent malic enzyme	ME1	Tricarboxylic acid cycle	Oxidoreductase activity
P21399	Cytoplasmic aconitate hydratase	ACO1		Oxidoreductase activity

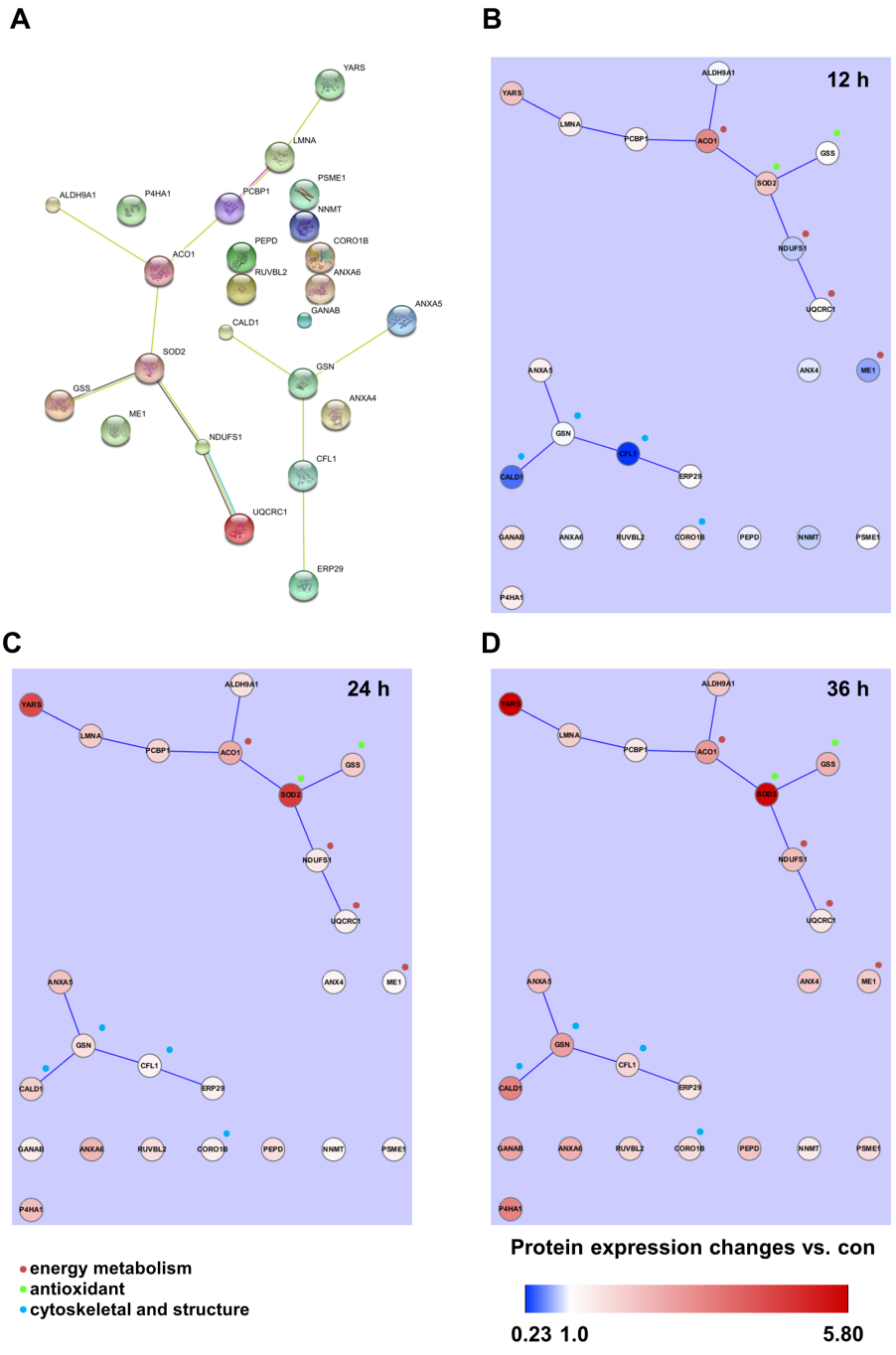

Fig. 3. Protein-protein interaction (PPI) analysis of identified proteins. (A) The functional cluster network was constructed using 13 experimentally identified proteins. PPI and time-dependent protein expression changes were mapped in the network. (B~D) LPS-treated time-dependent comparative protein expression changes were visualized using the Cytoscape program after LPS treatment for 12 h (B), 24 h (C), and 36 h (D). Color bar expresses the fold-change ratio (LPS treatment/Control). Molecular and Biological Function: ●: energy metabolism ● antioxidant ● cytoskeletal and structure.

differed in the groups that were treated with LPS for different times (12, 24, and 36 h) (Fig. 4A). The gene expression changes were highest in 12 h (998 up-regulated, 872 down-regulated). The number of commonly altered genes in all time points was 329 (up-regulated) and 369 (down-regulated) (Fig. 4A).

The results of the clustering of these genes are shown in Supplementary Fig. 3B. The top 10 upregulated or downregulated biological pathways in chondrocytes, treated with LPS for 36 h, were analyzed using a gene function enrichment analysis tool (Figs. 4B and C). The following upregulated biological pathways were identified: chemotaxis, hemopoietic or lymphoid organ development, positive regulation of cell proliferation, hemopoiesis, cell death, organ morphogenesis, angiogenesis, regulation of cytokine biosynthetic process, cytokine metabolic process, and leukocyte differentiation (Fig. 4B). The following downregulated biological pathways were identified: positive regulation of transferase activity; transcription; DNA-dependent; blood coagulation; RNA biosynthetic process; regulation of transcription; protein modification process; morphogenesis of embryonic epithelium; regulation of kinase activity; regulation of nucleobase, nucleoside, nucleotide, and nucleic acid metabolic processes; and protein kinase cascade (Fig. 4C).

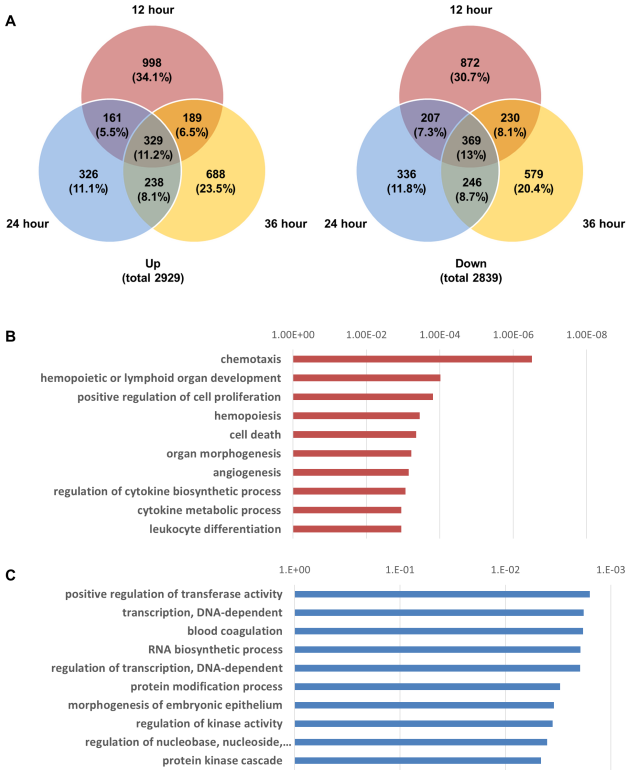

Fig. 4. Microarray results and biological pathway analysis in LPS-treated TLR-4-activated chondrocytes. (A) Venn diagram of up-regulated and down-regulated gene numbers in TLR-4 treated chondrocytes at 12, 24 and 36 h (B) Top 10 upregulated biological pathways in chondrocytes treated with LPS. (C) Top 10 downregulated biological pathways in chondrocytes treated with LPS.

Differentially expressed genes in cytokine-cytokine receptor interaction

Because the cytokine-cytokine receptor interactions play key role in the inflammation responses, we analyzed the time-dependent mRNA expression alterations in cytokine-cytokine receptor interaction map of the KEGG pathway.

The cytokine-cytokine receptor interaction map was classified by the sub-family of each cytokines including chemokine, hematopoietins, PDGF family, TNF family and TGF-β family. The results showed that 41 genes increased and 16 decreased in the 12-h LPS-treated chondrocytes, (Supplementary Fig. 5); 41 genes increased and 16 decreased in the 24-h and 40 genes increased and 18 decreased in 36-h LPS-treated chondrocytes, (Supplementary Figs. 6 and 7). The gene expression patterns in chemokines, PDGF family, TNF family and TGF-β family were relatively constant at all time points, however the time dependent changes of mRNA level in hematopoietins and its receptor were remarkably altered at 36 h (Fig. 5). At 36 h, mRNA expression pattern of interleukin 6 signal transducer (IL6ST) and interleukin 13 receptor subunit alpha 1 (IL13RA1) was reversed from the previous time points. In detail, the IL6ST expression was

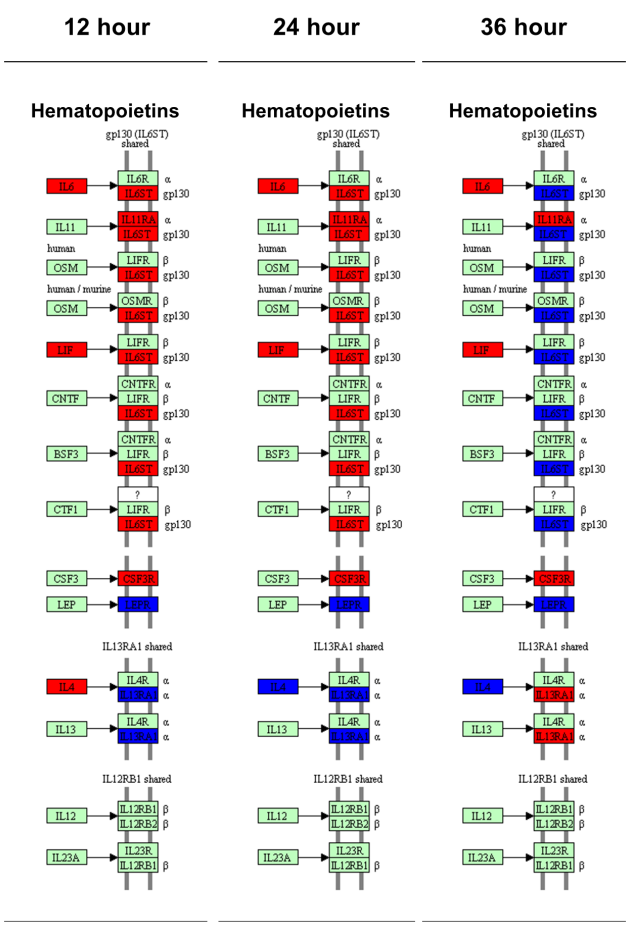

Fig. 5. Cytokine-cytokine receptor interaction pathway map in KEGG presented with relative gene expression of 12, 24 and 36 h vs. Con. Red: up-regulated genes, Blue: down-regulated genes, Green: unchanged genes.

decreased and IL13RA1 expression was increased than control group at 36 h (Fig. 5).

Comparison of proteomic and genomic results

We compared the results from 2DE proteomics and microarray genomics analyses, and identified nine pattern-matched proteins that displayed increased expression in both proteomics and genomics data (Supplementary Fig. 4). These nine proteins were NNMT, RUVBL2, ALDH9A1, ANXA6, PSME1, GSS, ACO1, LMNA, and SOD2.

Western blot confirmation of lamin A/C and annexin 4/5/6 expression

To confirm the proteomics and genomics results, the protein expression levels of lamin A/C and annexins were assessed in LPS-treated chondrocytes by performing western blot analysis. The results showed that lamin A/C expression was significantly

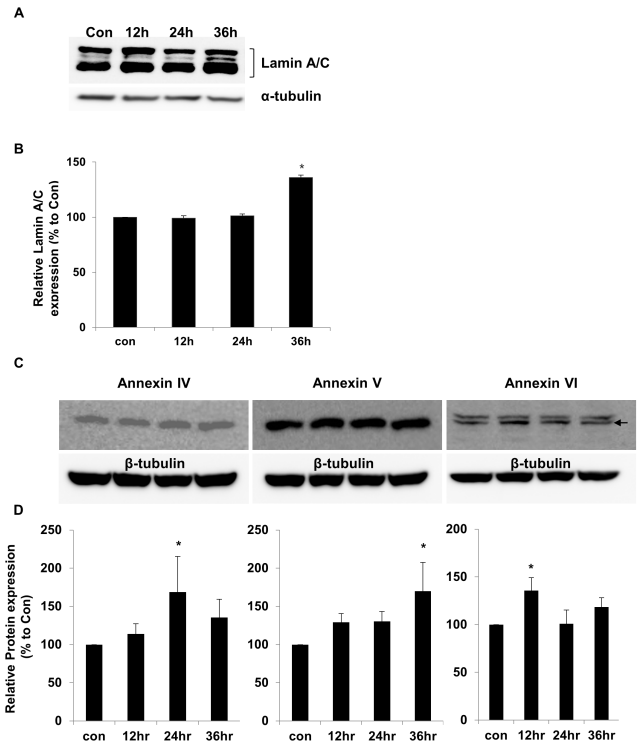

Fig. 6. Confirmation of lamin A/C and annexin expression by immunoblotting. (A) Representative immunoblot of lamin A/C expression in LPS-treated chondrocytes. (B) Histogram of untreated control (CON) chondrocytes and after LPS treatment for 12, 24, and 36 h to activate TLR-4 (*p<0.05). (C) Representative immunoblot of annexin 4/5/6 expression in LPS-treated chondrocytes. (D) Histogram of untreated control (CON) chondrocytes and after LPS treatment for 12, 24, and 36 h to activate TLR-4 (*p<0.05) (*n*=3).

higher (136±2.11%) after 36 h of LPS treatment than in controls (Fig. 6A). The relative lamin A/C expression levels are shown in Fig. 6B. The levels of annexin 4/5/6 expression also were investigated by performing western blot analysis (Fig. 6C). The relative expression levels of annexin 4/5/6 were significantly higher at 24, 36, and 12 h of LPS treatment, respectively (Fig. 6D). We used α-tubulin or β-tubulin as internal control standards for protein expression levels in control and TLR-4-activated chondrocytes.

DISCUSSION

LPS-mediated TLR-4 activation in chondrocytes

TLR has an important role in inducing immune and inflammatory responses [33]. LPS is commonly used to activate TLR-4. In this study, chondrocytes were treated with 1 μg/ml LPS to activate TLR-4, which consequently activated the NF-$_k$B signaling pathway and induced the synthesis and secretion of proinflammatory mediators such as IL-1/6/8 and TNF-α [34]. TNF is one of several important executors of the LPS-induced cytotoxic response [35]; it is known to be produced by nuclear translocation of NF-$_k$B [36].

Many in vivo and in vitro studies showed that IL-1 and TNF-α are major catabolic cytokines that destroy articular chondrocytes in rheumatoid arthritis [37-39]. Other studies showed that the cytokines IL-1, IL-6, and TNF-α are produced during the early phase of the TLR-4-mediated response [22]. To examine cytokine expression in LPS-treated chondrocytes, we performed real-time PCR analysis of cDNA synthesized from total RNA extracted from LPS-treated and control chondrocytes. The results showed that IL-β, IL-6, and TNF-α levels increased in chondrocytes treated with LPS for 12, 24, and 36 h. TNF-α increased 15 times, suggesting that this activated the downstream NF-$_k$B signaling pathway of TLR-4. These results indicate that LPS treatment activated TLR-4 and downstream inflammatory pathways in chondrocytes.

Proteomic alterations in LPS/TLR-4-activated chondrocytes

Proteomic analysis is a very effective method for comparing protein expression profiles in multiple target cells or tissues [40,41]. Of the 11 TLRs in humans, TLR-4 is the most extensively studied receptor [42]. Kim et al. [19] showed that the expression of TLR-2 and TLR-4 strongly increased in the cartilage of patients with osteoarthritis. Activation of TLR-2 and TLR-4 ligands strongly induced catabolism in chondrocytes. We performed 2DE proteomics analysis to compare TLR-4-mediated changes in protein expression levels in LPS-treated chondrocytes with those in controls. These results enabled us to determine TLR-4-mediated changes in the protein expression profiles in LPS-treated chondrocytes and the functional classifications and networks of these proteins. These functions can be divided into 11 groups. Two major alterations in functional networks were observed in the time-dependent network analysis (Fig. 3, Table 4). In the protein-protein interaction network, one functional module primarily related to mitochondrial energy metabolism (UQCRC1, NDUFS1, ACO1, and ME1) and antioxidant regulation (SOD2 and GSS). The other functional module primarily related to cytoskeletal or structural proteins (GSN, CALD1, CORO1B, and CFL1). Inflammation is a cellular process that is highly energy dependent and mediated by oxidative stress [43-45]. The cytoskeleton network, including coronin and cofilin-1, has an important role in inflammation and immune responses under both physiological and pathological conditions [46-48]. A recent study suggested that mitochondrial energy metabolism and ROS generation are strongly related to LPS/TLR-4-induced Nlrp3 inflammasome activation [45]. Thus, the time-dependent increased expression of those proteins could activate the functional networks and lead to LPS/TLR-4-induced inflammation of chondrocytes in our model system. These results are consistent with those reported in a previous atherosclerosis

model [49], which also observed a combination of energy metabolism and oxidative stress pathways in the proteomic response.

Genomic alterations in LPS/TLR-4-activated chondrocytes

We performed cDNA microarray analysis [50,51] to determine the changes in gene expression profiles in LPS/TLR-4-activated chondrocytes. Previous microarray analyses have investigated gene expression in tissues of patients with rheumatoid arthritis and osteoarthritis [52]. However, these studies have not determined TLR-4-induced changes in gene expression profiles in cartilage cells during the development of arthritis. Therefore, we used microarrays to collect these data during time-course experiments in LPS-treated chondrocytes. Unlike the observed changes at the protein level, which were mainly altered at 36 h, gene expression profiles changed most significantly when TLR-4 was activated with LPS for 12 h. At 12 h, 1,677 or 1740 genes underwent ≥2-fold increases or decreases, respectively. Among those genes, 998 (34.1%) of total up-regulated genes and 872 (30.7%) of total down-regulated genes were exclusively altered at 12 h (Fig. 4A).

Gene ontology analysis clearly showed the activation of essential pathways involved in inflammation, including chemotaxis, hematopoiesis, regulation of cytokine biosynthetic process, and cytokine metabolic process (Fig. 4B). Representative highly expressed genes responding to LPS/TLR-4-induced activation include the following: G-protein coupled receptor 111 (average 66-fold greater than control); Interleukin 8 (58-fold increase); serum amyloid A1 (33-fold increase); chemokines CXCL1, CXCL2, and CXCL3 (21-fold, 14-fold, and 10-fold increase, respectively); Claudin 1 (19-fold increase); 2',5'-oligoadenylae synthetase (13-fold increase); Progastricsin (12-fold increase); Interferon-inducible protein p78 (10-fold increase); and superoxide dismutase 2 (9-fold increase). Of the 2,839 genes that displayed reduced expression, 245 (4.70%) were involved in the GO pathway for the modulation of nucleobase, nucleoside, nucleotide, and nucleic acids (Fig. 4C). These genomic data provide valuable information about chondrocyte genes and cellular mechanisms targeted by TLR4 activation during the development of chondrocyte-mediated arthritis.

Cytokine plays an important role in immunity, infection, the hematogenous function, tissue repair, and the development and growth of cells. It particularly plays a major role in the immune system. Most of the immunologic functions involve more than one type of cytokine. LPS, a substance that induces bacterial inflammation, stimulates immunocytes via TLR-4. The activated immunocytes secrete various types of inflammation-inducing cytokines, and induce apoptosis and cell death. Cytokines can be divided into various families according to their structure or binding receptors.

To understand the inflammatory response that was induced in the chondrocytes, 62 genes that are involved in the cytokine-cytokine receptor interaction in the KEGG pathway were selected, and the change in the expression of such genes was examined on the KEGG pathway map. Unlike the relatively constant gene expression patterns in chemokines, PDGF family, TNF family and TGF-β family, mRNA level of cytokine receptors in hematopoietins were remarkably altered at 36 h. (Fig. 5). The mRNA expression of IL6ST was keep increased until 24 h but decreased at 36 h. In contrast, the expression of IL13RA1 was repressed until 24 h but increased at 35 h. IL6ST and IL13RA1 play important role in downstream activation of interleukins signaling pathways [53,54]. IL6ST is an important signal transducer which can be shared by interleukin 6 and 11 (IL6, 11), ciliary neurotrophic factor (CNTF), leukemia inhibitory factor (LIF), B-cell stimulating factor 3 (BSF3) and oncostatin M (OSM) [53]. IL13RA1 forms a receptor complex with IL4 receptor, which mediates the signaling processes of JAK1, STAT3 and STAT5 activation [54]. Interestingly, the gene expressions of major receptors (IL6R, LIFR, CNTFR, IL4R and OSMR) for those cytokines were comparable to control group all the time, however the expression of IL6ST and IL13RA1 had been altered dynamically (Fig. 5) which suggest the important regulatory role of these genes. These results suggested the existence of IL mediated temporal regulatory mechanism in the TLR-4 induced chondrocyte inflammation.

Lamin and annexin function in chondrocyte inflammation

Lamin A/C: Among the nine proteins with proteomic and genomic pattern matching, we performed western blot analysis to confirm increased expression of lamin A/C and annexin 4/5/6 in LPS-treated chondrocytes. Lamin A/C is a constituent of the cytoskeleton and is a type A lamin (there are two types of lamins, type A and type B) [55-57]. Lamin A/C maintains nuclear integrity and participates in nuclear membrane reformation after somatic cell division [58,59]. Helfand et al. reported that lamin is a type V intermediate fiber that is responsible for cellular shape and structure, and it localizes in the nucleus [60]. Helfand et al. also reported that lamin A/C localizes in the bone matrix, and lamin A/C expression declines as chondrocyte cells age in mice [56,60]. Our 2DE results indicate that lamin A/C expression increased in TLR-4-actived chondrocytes after LPS treatment for 24 or 36 h (Fig. 2). The increase in lamin A/C levels after LPS treatment for 36 h was confirmed with western blots (Fig. 6).

A 2DE proteomic study of chondrocytes from patients with osteoarthritis also reported increased expression of lamin A (type A) compared with control chondrocytes [61]. Several studies reported that lamin A/C affects chromatin organization, DNA replication, transcriptional regulation, and signal transduction [62,63]. Lamin proteolysis was observed in apoptotic cells

[64]. The cellular changes that occur during apoptosis are due to cleavage of cellular proteins such as lamin A/C and Poly (ADP-ribose) polymerase (PARP) [65-67]. When apoptosis is induced, lamin A/C is cut into small fragments of 29 kDa [68]. Mutations in the *lamin A* (*LmnA*) gene are related to diseases such as cardiomyopathy, lipodystrophy, and segmental premature aging syndrome [63]. A recent study suggested the important role of lamin A in aging and inflammation [69,70]. Mutation of *LmnA* increased the transcript levels of inflammatory markers in arteries, liver, and skin of mouse Hutchinson-Gilford progeria syndrome models, which suggested that changes in gene expression and gene mutation-induced posttranslational modification of lamin A are important in aging and inflammation [69,70]. Our results suggest that lamin A/C is involved in TLR-4 induced inflammation and chondrocyte cell death, which leads to the development and progression of arthritis. Future studies should analyze posttranscriptional modifications and perform functional validation of increased levels of lamin A/C during TLR-4 activation to clarify the role of lamin A/C in chondrocyte inflammation.

Annexins: Annexins are a family of membrane-binding proteins that share structural properties and biological activities associated with membrane-related processes. Members of the annexin family bind to negatively charged phospholipids in the presence of Ca^{2+}, and regulate important biological functions including vesicle trafficking, cell division, apoptosis, and growth regulation [71]. Changes in annexin expression and localization are implicated in diseases such as cancer, diabetes, and immune dysfunction [72,73]. Terminally differentiated hypertrophic chondrocytes release matrix vesicles containing annexins to the surrounding extracellular matrix; these annexins can initiate Ca^{2+} influx into matrix vesicles, thereby causing cartilage mineralization [74]. These results indicate that annexins have a fundamental role in bone and cartilage biology.

Annexin A1 is an anti-inflammatory protein that inhibits iNOS expression, cytochrome oxidase-2 activity, and cytokine-induced activation of phospholipase A2 (PLA2) [75]. Silencing of constitutively expressed annexin 1 significantly increases TNF-α and IL-6 production [76]. However, the present proteomic and genomic analyses did not detect changes in annexin A1 expression. Annexin 4 is a calcium/phospholipid-binding protein that promotes membrane fusion; it is involved in exocytosis and inhibits PLA2 [77,78]. Annexin 4 overexpression was reported in renal cell carcinoma and is related to anti-cancer drug resistance [72]. The relationship between annexin 4 and chondrocyte inflammation remains to be elucidated. Annexin 5 is an anticoagulant protein that acts as an indirect inhibitor of thromboplastin-specific complex and PLA2 [72,79]. Previous studies suggested an important roles for annexin 5 in the inflammation of tissues such as the heart, vascular endothelial cells, and lung, and in systemic sepsis [80-84]. Modifications in annexin 5 expression have been implicated in cardiovascular diseases [85], cancers [72], osteoarthritis [86], and rheumatoid arthritis [87]. Annexin 5 has important roles in chondrocyte adhesion, differentiation, and apoptosis [88-91]. Annexin 6, another calcium/phospholipid-binding protein, has been implicated in endosome aggregation and vesicle fusion; it is reported as a late differentiation marker for osteoarthritic chondrocytes [92]. Double deficiency of annexin 5 and 6 changes the transcriptome in growth plate cartilage, but does not induce any bone abnormality in the double-knockout mouse model [74]. These combined results suggest that increases in annexin 5 and 6 expression are important indicators of chondrocyte inflammation and osteoarthritis.

Although, there are independent studies demonstrated the increase or activation of TLR-4 [93], annexin 2, 5 and 6 [92,94] or lamin A/C [58] under the osteoarthritic conditions separately. However no study demonstrated expressional alteration of those components at same spatial and temporal condition yet. In the best of our knowledge, this is the first study demonstrated the increased expression of those annexins and lamin A/C under the TLR-4 activation condition. However further studies are needed to elucidate the underlying mechanism of between TLR-4 activation and increases of those key proteins.

CONCLUSION

In this study, we collected data on proteins and genes that showed distinct differences in LPS-treated chondrocytes and were closely related to the TLR-4-mediated inflammatory response leading to arthritis. These data demonstrate that the use of -omics analyses enable greater understanding of the molecular mechanisms involved in TLR-4-mediated chondrocyte inflammation and osteoarthritis.

ACKNOWLEDGEMENTS

This study was supported by grants from the Priority Research Centers Program and Basic Science Research Program through the National Research Foundation of Korea (NRF), funded by the Ministry of Education, Science, and Technology (2010-0020224, 2015R1A2A1A13001900 and 2015R1D1A1A01057937).

CONFLICTS OF INTEREST

The authors declare no conflicts of interest.

SUPPLEMENTARY MATERIALS

Supplementary data including seven figures can be found with

this article online at http://pdf.medrang.co.kr/paper/pdf/Kjpp/Kjpp021-05-07-s001.pdf.

REFERENCES

1. Sophia Fox AJ, Bedi A, Rodeo SA. The basic science of articular cartilage: structure, composition, and function. *Sports Health*. 2009;1:461-468.
2. Campo GM, Avenoso A, Campo S, D'Ascola A, Nastasi G, Calatroni A. Molecular size hyaluronan differently modulates toll-like receptor-4 in LPS-induced inflammation in mouse chondrocytes. *Biochimie*. 2010;92:204-215.
3. Sanchez-Adams J, Leddy HA, McNulty AL, O'Conor CJ, Guilak F. The mechanobiology of articular cartilage: bearing the burden of osteoarthritis. *Curr Rheumatol Rep*. 2014;16:451.
4. Gaston JS. Cytokines in arthritis--the 'big numbers' move centre stage. *Rheumatology* (*Oxford*). 2008;47:8-12.
5. Finckh A, Gabay C. At the horizon of innovative therapy in rheumatology: new biologic agents. *Curr Opin Rheumatol*. 2008;20:269-275.
6. McNulty AL, Moutos FT, Weinberg JB, Guilak F. Enhanced integrative repair of the porcine meniscus in vitro by inhibition of interleukin-1 or tumor necrosis factor alpha. *Arthritis Rheum*. 2007;56:3033-3042.
7. Homandberg GA, Hui F, Wen C. Fibronectin fragment mediated cartilage chondrolysis. I. Suppression by anti-oxidants. *Biochim Biophys Acta*. 1996;1317:134-142.
8. Hui W, Bell M, Carroll G. Oncostatin M (OSM) stimulates resorption and inhibits synthesis of proteoglycan in porcine articular cartilage explants. *Cytokine*. 1996;8:495-500.
9. Sandy JD, Neame PJ, Boynton RE, Flannery CR. Catabolism of aggrecan in cartilage explants. Identification of a major cleavage site within the interglobular domain. *J Biol Chem*. 1991;266:8683-8685.
10. Lai Y, Gallo RL. Toll-like receptors in skin infections and inflammatory diseases. *Infect Disord Drug Targets*. 2008;8:144-155.
11. O'Neill LA, Dinarello CA. The IL-1 receptor/toll-like receptor superfamily: crucial receptors for inflammation and host defense. *Immunol Today*. 2000;21:206-209.
12. Takeda K, Kaisho T, Akira S. Toll-like receptors. *Annu Rev Immunol*. 2003;21:335-376.
13. Beutler B, Jiang Z, Georgel P, Crozat K, Croker B, Rutschmann S, Du X, Hoebe K. Genetic analysis of host resistance: Toll-like receptor signaling and immunity at large. *Annu Rev Immunol*. 2006;24:353-389.
14. Bobacz K, Sunk IG, Hofstaetter JG, Amoyo L, Toma CD, Akira S, Weichhart T, Saemann M, Smolen JS. Toll-like receptors and chondrocytes: the lipopolysaccharide-induced decrease in cartilage matrix synthesis is dependent on the presence of toll-like receptor 4 and antagonized by bone morphogenetic protein 7. *Arthritis Rheum*. 2007;56:1880-1893.
15. Akira S, Uematsu S, Takeuchi O. Pathogen recognition and innate immunity. *Cell*. 2006;124:783-801.
16. Hughes AL, Piontkivska H. Functional diversification of the toll-like receptor gene family. *Immunogenetics*. 2008;60:249-256.
17. Liu-Bryan R, Terkeltaub R. Chondrocyte innate immune myeloid differentiation factor 88-dependent signaling drives procatabolic effects of the endogenous Toll-like receptor 2/Toll-like receptor 4 ligands low molecular weight hyaluronan and high mobility group box chromosomal protein 1 in mice. *Arthritis Rheum*. 2010;62:2004-2012.
18. Sillat T, Barreto G, Clarijs P, Soininen A, Ainola M, Pajarinen J, Korhonen M, Konttinen YT, Sakalyte R, Hukkanen M, Ylinen P, Nordström DC. Toll-like receptors in human chondrocytes and osteoarthritic cartilage. *Acta Orthop*. 2013;84:585-592.
19. Kim HA, Cho ML, Choi HY, Yoon CS, Jhun JY, Oh HJ, Kim HY. The catabolic pathway mediated by Toll-like receptors in human osteoarthritic chondrocytes. *Arthritis Rheum*. 2006;54:2152-2163.
20. Liu MH, Sun JS, Tsai SW, Sheu SY, Chen MH. Icariin protects murine chondrocytes from lipopolysaccharide-induced inflammatory responses and extracellular matrix degradation. *Nutr Res*. 2010;30:57-65.
21. Aota Y, An HS, Imai Y, Thonar EJ, Muehleman C, Masuda K. Comparison of cellular response in bovine intervertebral disc cells and articular chondrocytes: effects of lipopolysaccharide on proteoglycan metabolism. *Cell Tissue Res*. 2006;326:787-793.
22. Haglund L, Bernier SM, Onnerfjord P, Recklies AD. Proteomic analysis of the LPS-induced stress response in rat chondrocytes reveals induction of innate immune response components in articular cartilage. *Matrix Biol*. 2008;27:107-118.
23. Inada M, Matsumoto C, Uematsu S, Akira S, Miyaura C. Membrane-bound prostaglandin E synthase-1-mediated prostaglandin E2 production by osteoblast plays a critical role in lipopolysaccharide-induced bone loss associated with inflammation. *J Immunol*. 2006;177:1879-1885.
24. Matsuguchi T, Takagi K, Musikacharoen T, Yoshikai Y. Gene expressions of lipopolysaccharide receptors, toll-like receptors 2 and 4, are differently regulated in mouse T lymphocytes. *Blood*. 2000;95:1378-1385.
25. Pålsson-McDermott EM, O'Neill LA. Signal transduction by the lipopolysaccharide receptor, Toll-like receptor-4. *Immunology*. 2004;113:153-162.
26. Otero M, Goldring MB. Cells of the synovium in rheumatoid arthritis. Chondrocytes. *Arthritis Res Ther*. 2007;9:220.
27. Warda M, Kim HK, Kim N, Youm JB, Kang SH, Park WS, Khoa TM, Kim YH, Han J. Simulated hyperglycemia in rat cardiomyocytes: a proteomics approach for improved analysis of cellular alterations. *Proteomics*. 2007;7:2570-2590.
28. Pappin DJ, Hojrup P, Bleasby AJ. Rapid identification of proteins by peptide-mass fingerprinting. *Curr Biol*. 1993;3:327-332.
29. Heo HJ, Kim HK, Youm JB, Cho SW, Song IS, Lee SY, Ko TH, Kim N, Ko KS, Rhee BD, Han J. Mitochondrial pyruvate dehydrogenase phosphatase 1 regulates the early differentiation of cardiomyocytes from mouse embryonic stem cells. *Exp Mol Med*. 2016;48:e254.
30. Won KJ, Lin HY, Jung S, Cho SM, Shin HC, Bae YM, Lee SH, Kim HJ, Jeon BH, Kim B. Antifungal miconazole induces cardiotoxicity via inhibition of APE/Ref-1-related pathway in rat neonatal cardiomyocytes. *Toxicol Sci*. 2012;126:298-305.
31. Thu VT, Kim HK, Long le T, Thuy TT, Huy NQ, Kim SH, Kim N, Ko KS, Rhee BD, Han J. NecroX-5 exerts anti-inflammatory and anti-fibrotic effects via modulation of the TNFα/Dcn/TGFβ1/Smad2 pathway in hypoxia/reoxygenation-treated rat hearts. *Korean J Physiol Pharmacol*. 2016;20:305-314.

32. Huang SK, Darfler MM, Nicholl MB, You J, Bemis KG, Tegeler TJ, Wang M, Wery JP, Chong KK, Nguyen L, Scolyer RA, Hoon DS. LC/MS-based quantitative proteomic analysis of paraffin-embedded archival melanomas reveals potential proteomic biomarkers associated with metastasis. *PLoS One.* 2009;4:e4430.
33. Kim KH. Innate immunity and toll like receptors. *Korean J Pediatr.* 2004;47:6-11.
34. Schletter J, Heine H, Ulmer AJ, Rietschel ET. Molecular mechanisms of endotoxin activity. *Arch Microbiol.* 1995;164:383-389.
35. Beutler B, Milsark IW, Cerami AC. Passive immunization against cachectin/tumor necrosis factor protects mice from lethal effect of endotoxin. *Science.* 1985;229:869-871.
36. Shakhov AN, Collart MA, Vassalli P, Nedospasov SA, Jongeneel CV. Kappa B-type enhancers are involved in lipopolysaccharide-mediated transcriptional activation of the tumor necrosis factor alpha gene in primary macrophages. *J Exp Med.* 1990;171:35-47.
37. Huh YH, Lee G, Song WH, Koh JT, Ryu JH. Crosstalk between FLS and chondrocytes is regulated by HIF-2α-mediated cytokines in arthritis. *Exp Mol Med.* 2015;47:e197.
38. van den Berg WB. Animal models of arthritis. What have we learned? *J Rheumatol Suppl*. 2005;72:7-9.
39. van den Berg WB, van Riel PL. Uncoupling of inflammation and destruction in rheumatoid arthritis: myth or reality? *Arthritis Rheum.* 2005;52:995-999.
40. Dasuri K, Antonovici M, Chen K, Wong K, Standing K, Ens W, El-Gabalawy H, Wilkins JA. The synovial proteome: analysis of fibroblast-like synoviocytes. *Arthritis Res Ther.* 2004;6:R161-168.
41. Gillette MA, Carr SA. Quantitative analysis of peptides and proteins in biomedicine by targeted mass spectrometry. *Nat Methods.* 2013;10:28-34.
42. Gu S, Wang T, Chen X. Quantitative proteomic analysis of LPS-induced differential immune response associated with TLR4 Polymorphisms by multiplex amino acid coded mass tagging. *Proteomics*. 2008;8:3061-3070.
43. Wang H, Ye J. Regulation of energy balance by inflammation: common theme in physiology and pathology. *Rev Endocr Metab Disord.* 2015;16:47-54.
44. Ye J, Keller JN. Regulation of energy metabolism by inflammation: a feedback response in obesity and calorie restriction. *Aging* (*Albany NY*). 2010;2:361-368.
45. Lamkanfi M, Dixit VM. Mechanisms and functions of inflammasomes. *Cell.* 2014;157:1013-1022.
46. Rogers KR, Morris CJ, Blake DR. The cytoskeleton and its importance as a mediator of inflammation. *Ann Rheum Dis.* 1992;51:565-571.
47. Kopecki Z, Ludwig RJ, Cowin AJ. Cytoskeletal regulation of inflammation and its impact on skin blistering disease epidermolysis bullosa acquisita. *Int J Mol Sci.* 2016;17:E1116.
48. Wickramarachchi DC, Theofilopoulos AN, Kono DH. Immune pathology associated with altered actin cytoskeleton regulation. *Autoimmunity*. 2010;43:64-75.
49. Mayr M, Chung YL, Mayr U, Yin X, Ly L, Troy H, Fredericks S, Hu Y, Griffiths JR, Xu Q. Proteomic and metabolomic analyses of atherosclerotic vessels from apolipoprotein E-deficient mice reveal alterations in inflammation, oxidative stress, and energy metabolism. *Arterioscler Thromb Vasc Biol.* 2005;25:2135-2142.
50. Aigner T, Zien A, Hanisch D, Zimmer R. Gene expression in chondrocytes assessed with use of microarrays. *J Bone Joint Surg Am.* 2003;85-A Suppl 2:117-123.
51. Eisen MB, Spellman PT, Brown PO, Botstein D. Cluster analysis and display of genome-wide expression patterns. *Proc Natl Acad Sci U S A.* 1998;95:14863-14868.
52. Devauchelle V, Marion S, Cagnard N, Mistou S, Falgarone G, Breban M, Letourneur F, Pitaval A, Alibert O, Lucchesi C, Anract P, Hamadouche M, Ayral X, Dougados M, Gidrol X, Fournier C, Chiocchia G. DNA microarray allows molecular profiling of rheumatoid arthritis and identification of pathophysiological targets. *Genes Immun.* 2004;5:597-608.
53. Hibi M, Murakami M, Saito M, Hirano T, Taga T, Kishimoto T. Molecular cloning and expression of an IL-6 signal transducer, gp130. *Cell.* 1990;63:1149-1157.
54. Sheikh F, Dickensheets H, Pedras-Vasconcelos J, Ramalingam T, Helming L, Gordon S, Donnelly RP. The interleukin-13 receptor-α1 chain is essential for induction of the alternative macrophage activation pathway by IL-13 but not IL-4. *J Innate Immun.* 2015;7:494-505.
55. Dahl KN, Ribeiro AJ, Lammerding J. Nuclear shape, mechanics, and mechanotransduction. *Circ Res.* 2008;102:1307-1318.
56. Duque G, Rivas D. Age-related changes in lamin A/C expression in the osteoarticular system: laminopathies as a potential new aging mechanism. *Mech Ageing Dev.* 2006;127:378-383.
57. Smith ED, Kudlow BA, Frock RL, Kennedy BK. A-type nuclear lamins, progerias and other degenerative disorders. *Mech Ageing Dev.* 2005;126:447-460.
58. Attur M, Ben-Artzi A, Yang Q, Al-Mussawir HE, Worman HJ, Palmer G, Abramson SB. Perturbation of nuclear lamin A causes cell death in chondrocytes. *Arthritis Rheum.* 2012;64:1940-1949.
59. Hishiya A, Watanabe K. Progeroid syndrome as a model for impaired bone formation in senile osteoporosis. *J Bone Miner Metab.* 2004;22:399-403.
60. Helfand BT, Chang L, Goldman RD. Intermediate filaments are dynamic and motile elements of cellular architecture. *J Cell Sci.* 2004;117:133-141.
61. Ruiz-Romero C, Carreira V, Rego I, Remeseiro S, López-Armada MJ, Blanco FJ. Proteomic analysis of human osteoarthritic chondrocytes reveals protein changes in stress and glycolysis. *Proteomics*. 2008;8:495-507.
62. Miranda M, Chacón MR, Vidal F, Megia A, Richart C, Veloso S, Saumoy M, Olona C, Vendrell J. LMNA messenger RNA expression in highly active antiretroviral therapy-treated HIV-positive patients. *J Acquir Immune Defic Syndr.* 2007;46:384-389.
63. Tran JR, Chen H, Zheng X, Zheng Y. Lamin in inflammation and aging. *Curr Opin Cell Biol.* 2016;40:124-130.
64. Orth K, Chinnaiyan AM, Garg M, Froelich CJ, Dixit VM. The CED-3/ICE-like protease Mch2 is activated during apoptosis and cleaves the death substrate lamin A. *J Biol Chem.* 1996;271:16443-16446.
65. Alnemri ES, Livingston DJ, Nicholson DW, Salvesen G, Thornberry NA, Wong WW, Yuan J. Human ICE/CED-3 protease nomenclature. *Cell.* 1996;87:171.
66. Kaufmann SH, Desnoyers S, Ottaviano Y, Davidson NE, Poirier GG. Specific proteolytic cleavage of poly(ADP-ribose) polymerase: an early marker of chemotherapy-induced apoptosis. *Cancer Res.* 1993;53:3976-3985.

67. Zhuang J, Dinsdale D, Cohen GM. Apoptosis, in human monocytic THP.1 cells, results in the release of cytochrome c from mitochondria prior to their ultracondensation, formation of outer membrane discontinuities and reduction in inner membrane potential. *Cell Death Differ.* 1998;5:953-962.
68. Okinaga T, Kasai H, Tsujisawa T, Nishihara T. Role of caspases in cleavage of lamin A/C and PARP during apoptosis in macrophages infected with a periodontopathic bacterium. *J Med Microbiol.* 2007;56:1399-1404.
69. Osorio FG, Bárcena C, Soria-Valles C, Ramsay AJ, de Carlos F, Cobo J, Fueyo A, Freije JM, López-Otín C. Nuclear lamina defects cause ATM-dependent NF-κB activation and link accelerated aging to a systemic inflammatory response. *Genes Dev.* 2012;26:2311-2324.
70. McKenna T, Rosengardten Y, Viceconte N, Baek JH, Grochová D, Eriksson M. Embryonic expression of the common progeroid lamin A splice mutation arrests postnatal skin development. *Aging Cell.* 2014;13:292-302.
71. Gerke V, Creutz CE, Moss SE. Annexins: linking Ca^{2+} signalling to membrane dynamics. *Nat Rev Mol Cell Biol.* 2005;6:449-461.
72. Hayes MJ, Moss SE. Annexins and disease. *Biochem Biophys Res Commun.* 2004;322:1166-1170.
73. Fatimathas L, Moss SE. Annexins as disease modifiers. *Histol Histopathol.* 2010;25:527-532.
74. Belluoccio D, Grskovic I, Niehoff A, Schlötzer-Schrehardt U, Rosenbaum S, Etich J, Frie C, Pausch F, Moss SE, Pöschl E, Bateman JF, Brachvogel B. Deficiency of annexins A5 and A6 induces complex changes in the transcriptome of growth plate cartilage but does not inhibit the induction of mineralization. *J Bone Miner Res.* 2010;25:141-153.
75. Kim SW, Rhee HJ, Ko J, Kim YJ, Kim HG, Yang JM, Choi EC, Na DS. Inhibition of cytosolic phospholipase A2 by annexin I. Specific interaction model and mapping of the interaction site. *J Biol Chem.* 2001;276:15712-15719.
76. Jia Y, Morand EF, Song W, Cheng Q, Stewart A, Yang YH. Regulation of lung fibroblast activation by annexin A1. *J Cell Physiol.* 2013;228:476-484.
77. Zanotti G, Malpeli G, Gliubich F, Folli C, Stoppini M, Olivi L, Savoia A, Berni R. Structure of the trigonal crystal form of bovine annexin IV. *Biochem J.* 1998;329:101-106.
78. Hauptmann R, Maurer-Fogy I, Krystek E, Bodo G, Andree H, Reutelingsperger CP. Vascular anticoagulant beta: a novel human Ca^{2+}/phospholipid binding protein that inhibits coagulation and phospholipase A2 activity. Its molecular cloning, expression and comparison with VAC-alpha. *Eur J Biochem.* 1989;185:63-71.
79. Mira JP, Dubois T, Oudinet JP, Lukowski S, Russo-Marie F, Geny B. Inhibition of cytosolic phospholipase A2 by annexin V in differentiated permeabilized HL-60 cells. Evidence of crucial importance of domain I type II Ca^{2+}-binding site in the mechanism of inhibition. *J Biol Chem.* 1997;272:10474-10482.
80. Reutelingsperger CP, van Heerde WL. Annexin V, the regulator of phosphatidylserine-catalyzed inflammation and coagulation during apoptosis. *Cell Mol Life Sci.* 1997;53:527-532.
81. Tokita N, Hasegawa S, Maruyama K, Izumi T, Blankenberg FG, Tait JF, Strauss HW, Nishimura T. 99mTc-Hynic-annexin V imaging to evaluate inflammation and apoptosis in rats with autoimmune myocarditis. *Eur J Nucl Med Mol Imaging.* 2003;30:232-238.
82. Ewing MM, de Vries MR, Nordzell M, Pettersson K, de Boer HC, van Zonneveld AJ, Frostegård J, Jukema JW, Quax PH. Annexin A5 therapy attenuates vascular inflammation and remodeling and improves endothelial function in mice. *Arterioscler Thromb Vasc Biol.* 2011;31:95-101.
83. Park JH, Jang JH, Choi EJ, Kim YS, Lee EJ, Jung ID, Han HD, Wu TC, Hung CF, Kang TH, Park YM. Annexin A5 increases survival in murine sepsis model by inhibiting HMGB1-mediated pro-inflammation and coagulation. *Mol Med.* 2016;22.
84. Buckley S, Shi W, Xu W, Frey MR, Moats R, Pardo A, Selman M, Warburton D. Increased alveolar soluble annexin V promotes lung inflammation and fibrosis. *Eur Respir J.* 2015;46:1417-1429.
85. Ravassa S, González A, López B, Beaumont J, Querejeta R, Larman M, Díez J. Upregulation of myocardial Annexin A5 in hypertensive heart disease: association with systolic dysfunction. *Eur Heart J.* 2007;28:2785-2791.
86. Mollenhauer J, Mok MT, King KB, Gupta M, Chubinskaya S, Koepp H, Cole AA. Expression of anchorin CII (cartilage annexin V) in human young, normal adult, and osteoarthritic cartilage. *J Histochem Cytochem.* 1999;47:209-220.
87. Rodríguez-García MI, Fernández JA, Rodríguez A, Fernández MP, Gutierrez C, Torre-Alonso JC. Annexin V autoantibodies in rheumatoid arthritis. *Ann Rheum Dis.* 1996;55:895-900.
88. Kim HJ, Kirsch T. Collagen/annexin V interactions regulate chondrocyte mineralization. *J Biol Chem.* 2008;283:10310-10317.
89. Ea HK, Monceau V, Camors E, Cohen-Solal M, Charlemagne D, Lioté F. Annexin 5 overexpression increased articular chondrocyte apoptosis induced by basic calcium phosphate crystals. *Ann Rheum Dis.* 2008;67:1617-1625.
90. Kurtis MS, Tu BP, Gaya OA, Mollenhauer J, Knudson W, Loeser RF, Knudson CB, Sah RL. Mechanisms of chondrocyte adhesion to cartilage: role of beta1-integrins, CD44, and annexin V. *J Orthop Res.* 2001;19:1122-1130.
91. Turnay J, Olmo N, Lizarbe MA, von der Mark K. Changes in the expression of annexin A5 gene during in vitro chondrocyte differentiation: influence of cell attachment. *J Cell Biochem.* 2001;84:132-142.
92. Pfander D, Swoboda B, Kirsch T. Expression of early and late differentiation markers (proliferating cell nuclear antigen, syndecan-3, annexin VI, and alkaline phosphatase) by human osteoarthritic chondrocytes. *Am J Pathol.* 2001;159:1777-1783.
93. Gómez R, Villalvilla A, Largo R, Gualillo O, Herrero-Beaumont G. TLR4 signalling in osteoarthritis–finding targets for candidate DMOADs. *Nat Rev Rheumatol.* 2015;11:159-170.
94. Kirsch T, Swoboda B, Nah H. Activation of annexin II and V expression, terminal differentiation, mineralization and apoptosis in human osteoarthritic cartilage. *Osteoarthritis Cartilage.* 2000;8:294-302.

Online Supplementary Materials

1. Supplementary Method

Two-dimensional gel electrophoresis

1. Protein sample preparation

Harvest chondrocytes pellets were washed twice with ice-cold PBS (in molecular cloning) and sonicated for 10 seconds by Sonoplus (Bandelin electronic, Berlin, Germany), in sample lysis solution composed with 7 M urea, 2 M Thiourea containing 4%(w/v) 3-[(3-cholamidopropy) dimethyammonio]-1-propanesulfonate (CHAPS), 1%(w/v) dithiothreitol (DTT) and 2% (v/v) pharmalyte and 1 mM benzamidine. Proteins were extracted for one hour at room temperature with vortexing. After centrifugation at 15,000xg for one hour at 15°C, insoluble material was discarded and soluble fraction was used for two-dimensional gel electrophoresis. Protein loading was normalized by Bradford assay [27].

2. Two dimensional electrophoresis (2DE)

Immobilized pH gradient (IPG) dry strips were equilibrated for 12-16 hours with 7 M urea, 2 M thiourea containing 2% 3-[(3-cholamidopropy) dimethyammonio]-1-propanesulfonate (CHAPS), 1% dithiothreitol (DTT), 1% pharmalyte and respectively loaded with 200 μg of sample. Isoelectric focusing (IEF) was performed at 20°C using a Multiphor II electrophoresis unit and EPS 3500 XL power supply (Amersham Biosciences, Little Chalfont, UK) following manufacturer's instruction. For IEF, the voltage was linearly increased from 150 to 3,500 V during 3 hours for sample entry followed by constant 3,500 V, with focusing complete after 96 kVh. Prior to the second dimension, strips were incubated for 10 minutes in equilibration buffer (50 mM Tris-Cl, pH 6.8 containing 6 M urea, 2% SDS and 30% glycerol), first with 1% DTT and second with 2.5% iodoacetamide. Equilibrated strips were inserted onto SDS-PAGE gels (20×24 cm, 10~16%). SDS-PAGE was performed using Hoefer DALT 2D system (Amersham Biosciences, Little Chalfont, UK) following manufacturer's instruction. 2D gels were run at 20°C for 1.7 kVh. And then 2D gels were silver stained as described by Oakley et al. [28] but fixing and sensitization step with glutaraldehyde was omitted.

3. Image analysis

Quantitative analysis of digitized images was carried out using the PDQuest (version 7.0, BioRad, Hercules, CA) software according to the protocols provided by the manufacturer. Quantity of each spot was normalized by total valid spot intensity. Protein spots were selected for the significant expression variation deviated over two fold in its expression level compared with control or normal sample.

4. Enzymatic digestion of protein in-gel

Protein spots were enzymatically digested in-gel in a manner similar to that previously described by Shevchenko et al [29] and using modified porcine trypsin. Gel pieces were washed with 50% acetonitrile to remove SDS, salt and stain, dried to remove solvent and then rehydrated with trypsin (8~10 ng/μl) and incubated 8~10 h at 37°C. The proteolytic reaction was terminated by addition of 5 μl 0.5% trifluoroacetic acid. Tryptic peptides were recovered by combining the aqueous phase from several extractions of gel pieces with 50% aqueous acetonitrile. After concentration the peptide mixture was desalted using C_{18}ZipTips (Millipore, Billerica, MA), and peptides eluted in 1~5 μl of acetonitrile. An aliquot of this solution was mixed with an equal volume of a saturated solution of α-cyano-4-hydroxycinnamic acid in 50% aqueous acetonitrile, and 1 μl of mixture spotted onto a target plate.

5. MALDI-TOF analysis and database search

Protein identifications were performed using an Ettan Matrix-assisted laser desorption/ionzation-time of flight mass spectrometry (MALDI-TOF) (Amersham Biosciences, Little Chalfont, UK). Peptides were evaporated with a N2 laser at 337 nm and using a delayed extraction approach. They were accelerated with 20 Kv injection pulse for time of flight analysis. Each spectrum was the cumulative average of 300 laser shots. The search program MASCOT (http://www.matrixscience.com/cgi/search_form.pl?FORMVER= 2&SEARCH=PMF) was used for protein identification by peptide mass fingerprinting. Spectra were calibrated with trypsin auto-digestion ion peak *m/z* (842.510, 2211.1046) as internal standards.

Microarray Genomics

1. RNA isolation and quality measurement

Total RNA of each sample was isolated by using the Qiaquick RNeasy Mini kit (Qiagen, Valencia, CA) according to the manufacturer's instructions. Briefly, each sample lysed in the Lysis buffer by repetitive pipetting and then 1 volume of 70% EtOH was added and mixed immediately by pipetting. The mixture was transferred to an RNeasy mini column and centrifuged at 12,000×g for 15 seconds.

350 μl of Buffer RW1 was added to the column and treated with RNase-free DNase to digest contaminating genomic DNA. Samples were washed by adding another 350 μl of Buffer RW1 and the column was washed with 500 μl of Buffer RPE two times. Eluted total RNA was quantified using a ND-1000 spectrophotometer

(NanoDrop Technologies, Inc., Wilmington, DE). The quality of the RNA was verified by an Agilent 2100 Bioanalyzer (Agilent Technologies, Palo Alto, CA).

2. Microarray analysis

For control and test RNAs, the synthesis of target cRNA probes and hybridization were performed using Agilent's Low RNA Input Linear Amplification kit (Agilent Technology, Santa Clara, CA, USA) according to the manufacturer's instructions. Briefly, each 1 ug total RNA and T7 promoter primer mix and incubated at 65oC for 10 min. cDNA master mix (5× First strand buffer, 0.1 M DTT, 10 mM dNTP mix, RNase-Out, and MMLV-RT) was prepared and added to the reaction mixer. The samples were incubated at 40°C for 2 hours and then the RT and dsDNA synthesis was terminated by incubating at 65°C for 15 min. The transcription master mix was prepared as the manufacturer's protocol (4× Transcription buffer, 0.1 M DTT, NTP mix, 50% PEG, RNase-Out, Inorganic pyrophosphatase, T7-RNA polymerase, and Cyanine 3/5-CTP). Transcription of dsDNA was preformed by adding the transcription master mix to the dsDNA reaction samples and incubating at 40°C for 2 hours. Amplified and labeled cRNA was purified on cRNA Cleanup Module (Agilent Technology, Santa Clara, CA, USA) according to the manufacturer's protocol. Labeled cRNA target was quantified using ND-1000 spectrophotometer (NanoDrop Technologies, Inc., Wilmington, DE). After checking labeling efficiency, fragmentation of cRNA was performed by adding 10× blocking agent and 25 × fragmentation buffers and incubating at 60°C for 30 min. The fragmented cRNA was resuspended with 2× hybridization buffer and directly pipetted onto assembled Agilent's Whole Human Genome Oligo Microarray (44K). The arrays hybridized at 65°C for 17 hours using Agilent Hybridization oven (Agilent Technology, Santa Clara, CA, USA). The hybridized microarrays were washed as the manufacturer's washing protocol (Agilent Technology, Santa Clara, CA, USA).

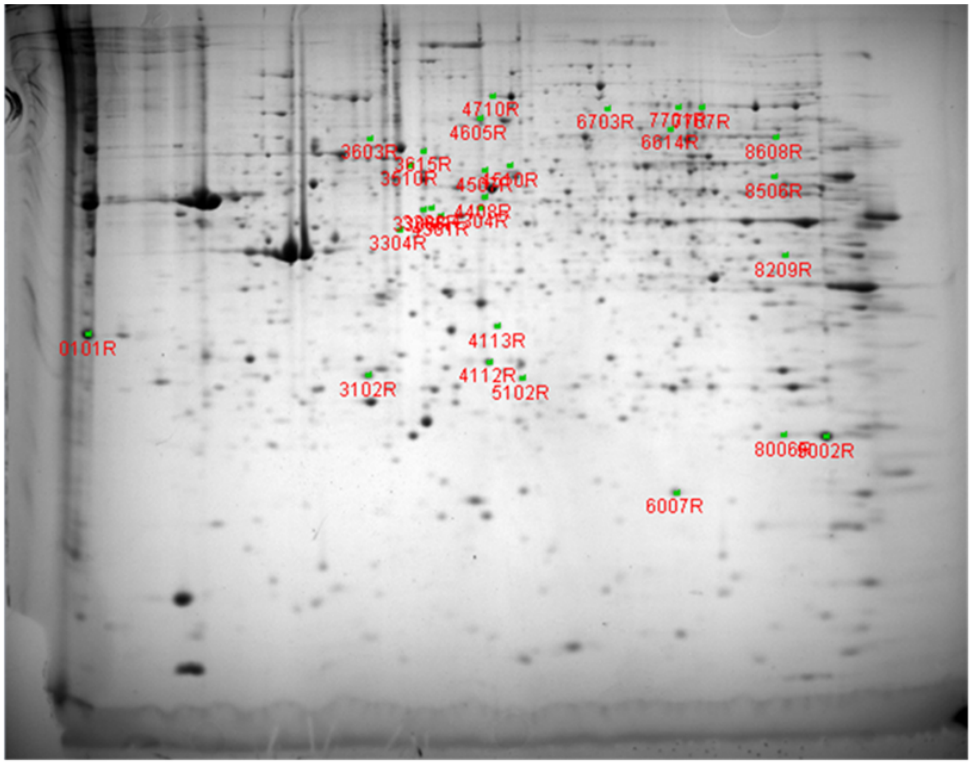

Supplementary Fig. 1. Representative 2DE gel images which is marked with selected spots.

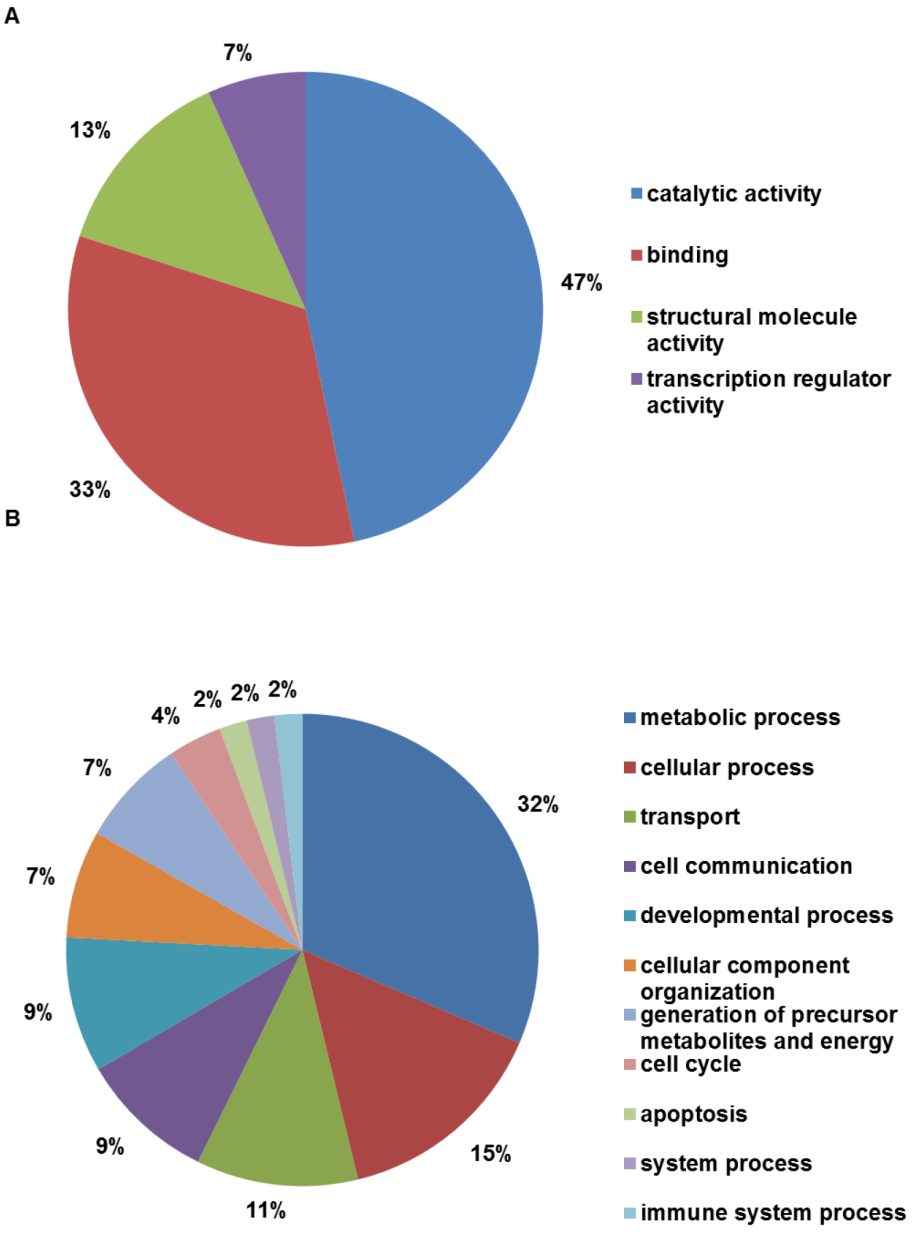

Supplementary Fig. 2. PANTHER classification of molecular function (A) and biological processes (B) of identified proteins.

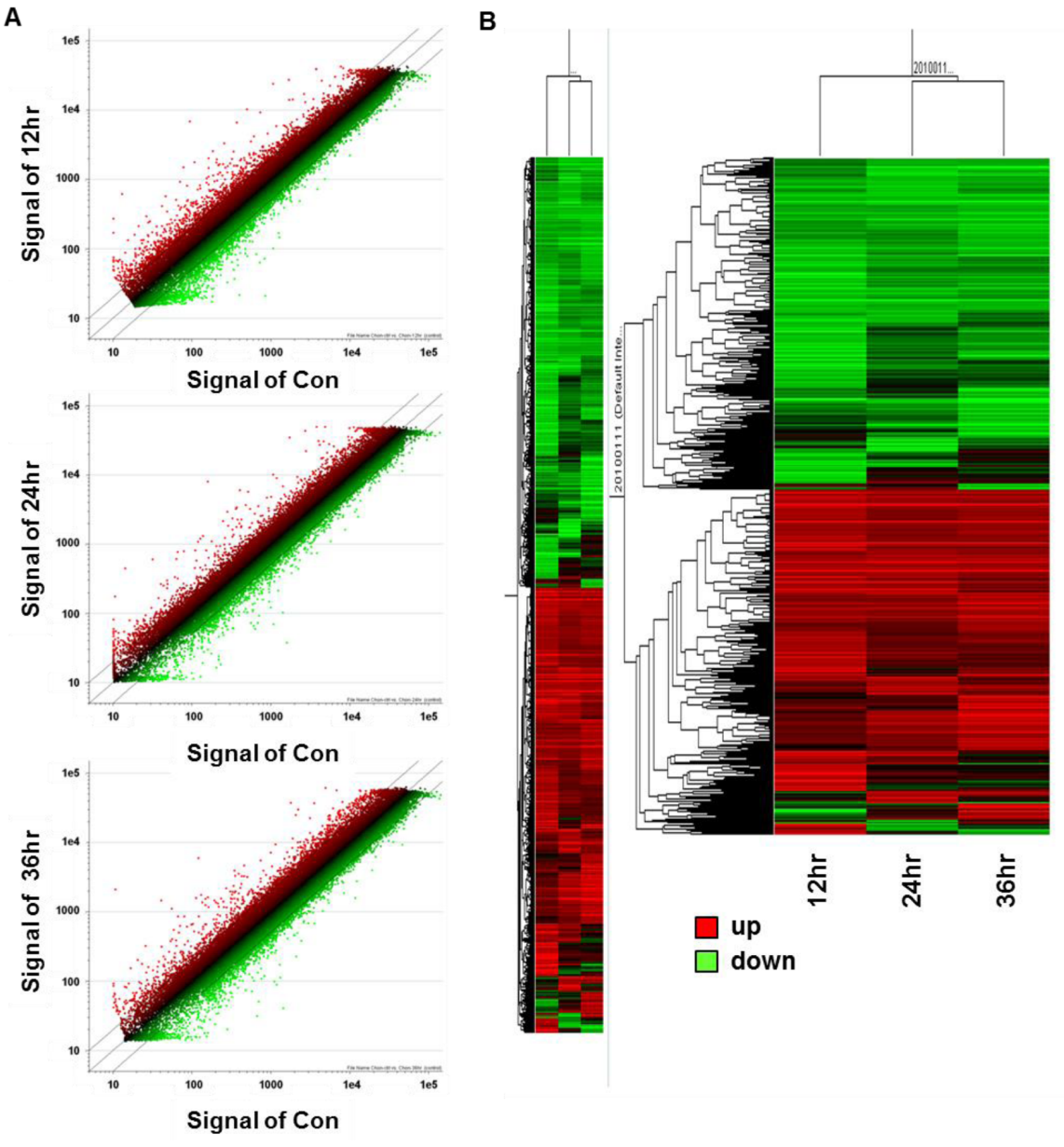

Supplementary Fig. 3. DNA expression chip microarray. (A) Scatter plot analysis for quantification and statistical analysis of each set. 12 hr-Con (top), 24 hr-Con (middle) and 36 hr-Con (bottom). (B) Gene clustering heat map.

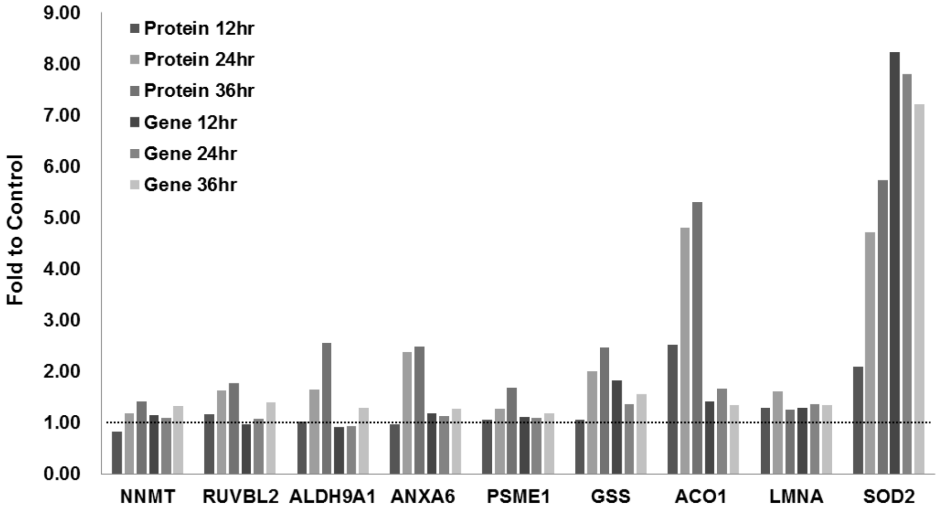

Supplementary Fig. 4. Comparison of proteomics and genomics results. Histogram of relative expression of protein or gene at the different time point of LPS-treated chondrocytes.

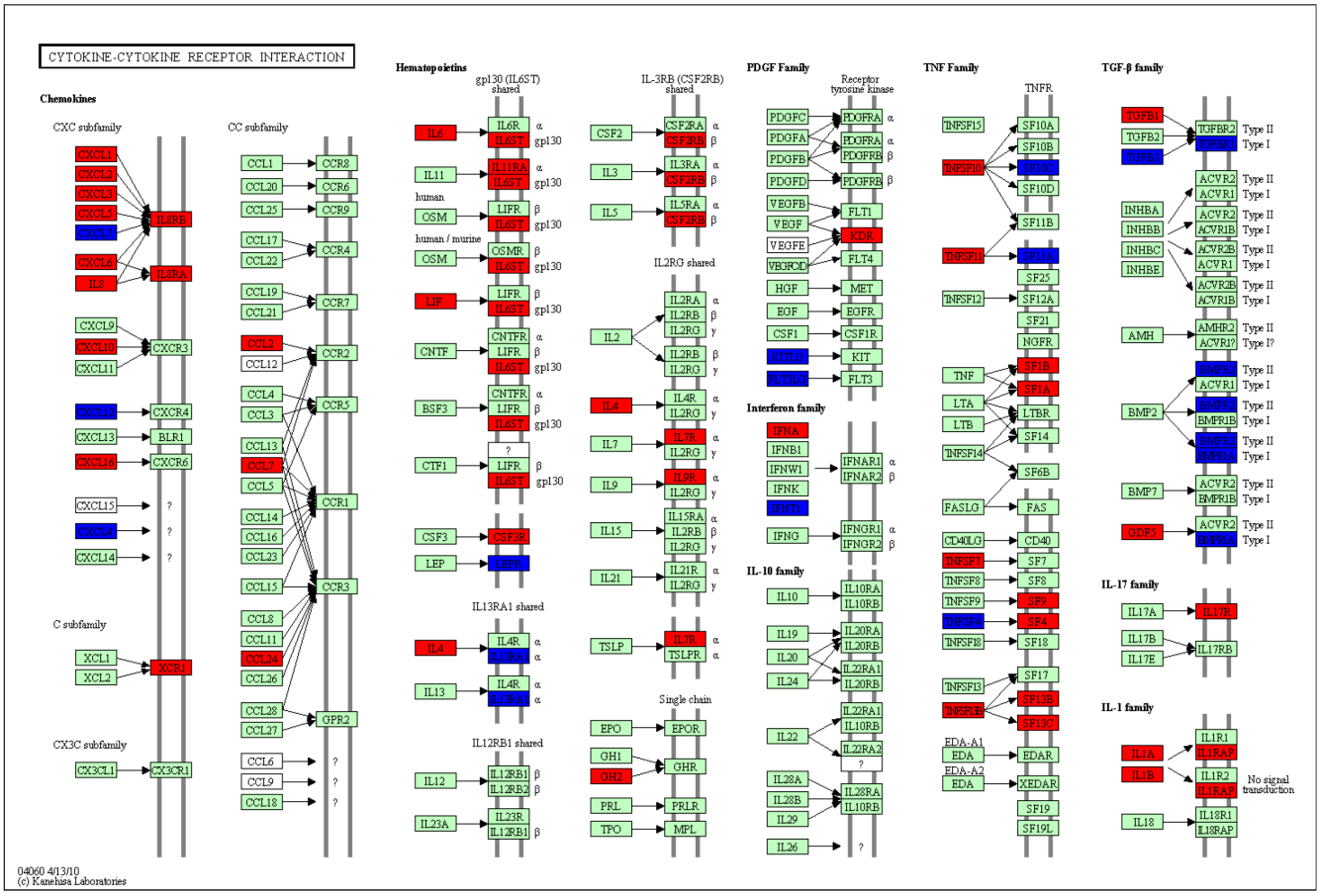

Supplementary Fig. 5. Cytokine-cytokine receptor interaction pathway map in KEGG presented with relative gene expression of 12 hr/Con.
Red: up-regulated genes, Blue: down-regulated genes, Green: unchanged genes.

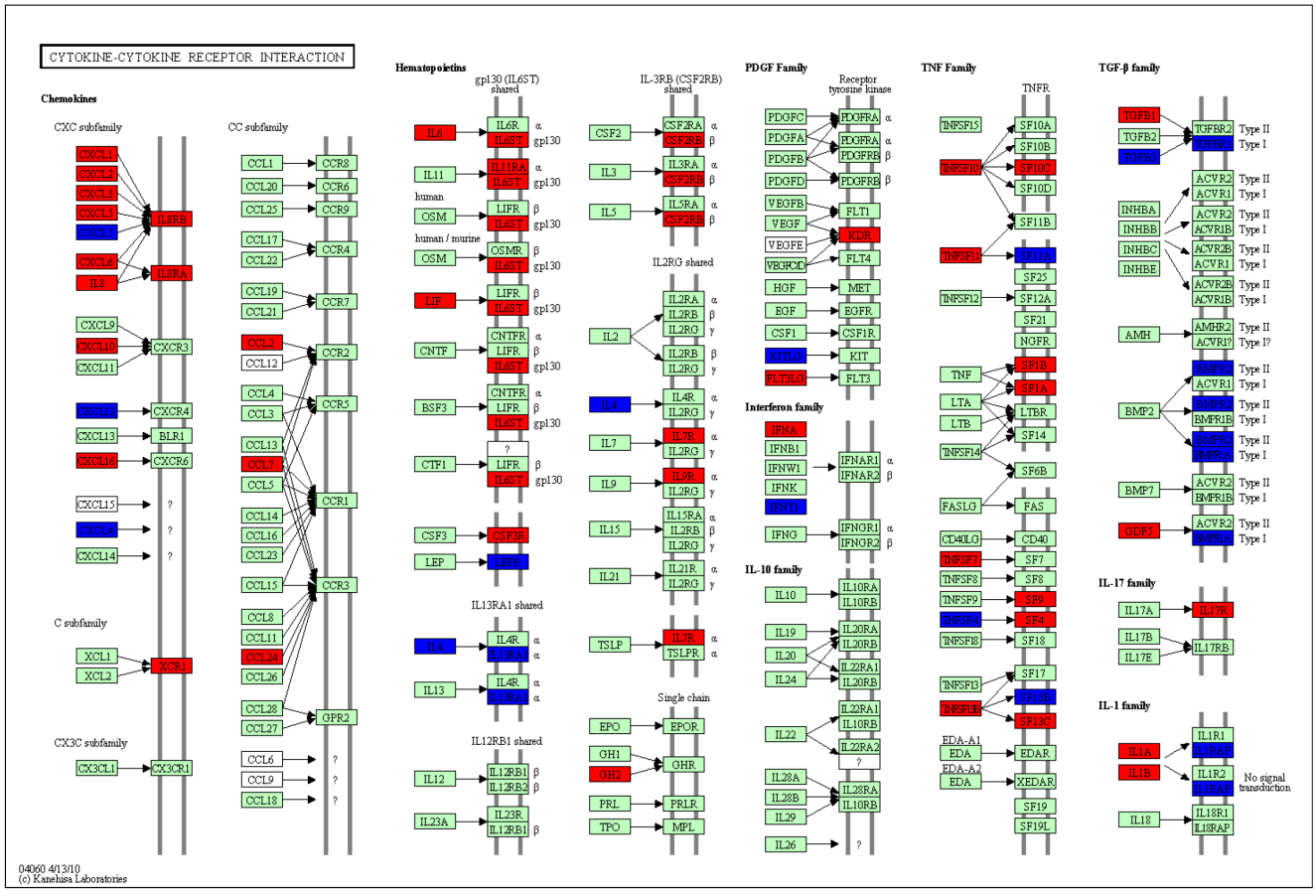

Supplementary Fig. 6. Cytokine-cytokine receptor interaction pathway map in KEGG presented with relative gene expression of 24 hr/Con.
Red: up-regulated genes, Blue: down-regulated genes, Green: unchanged genes.

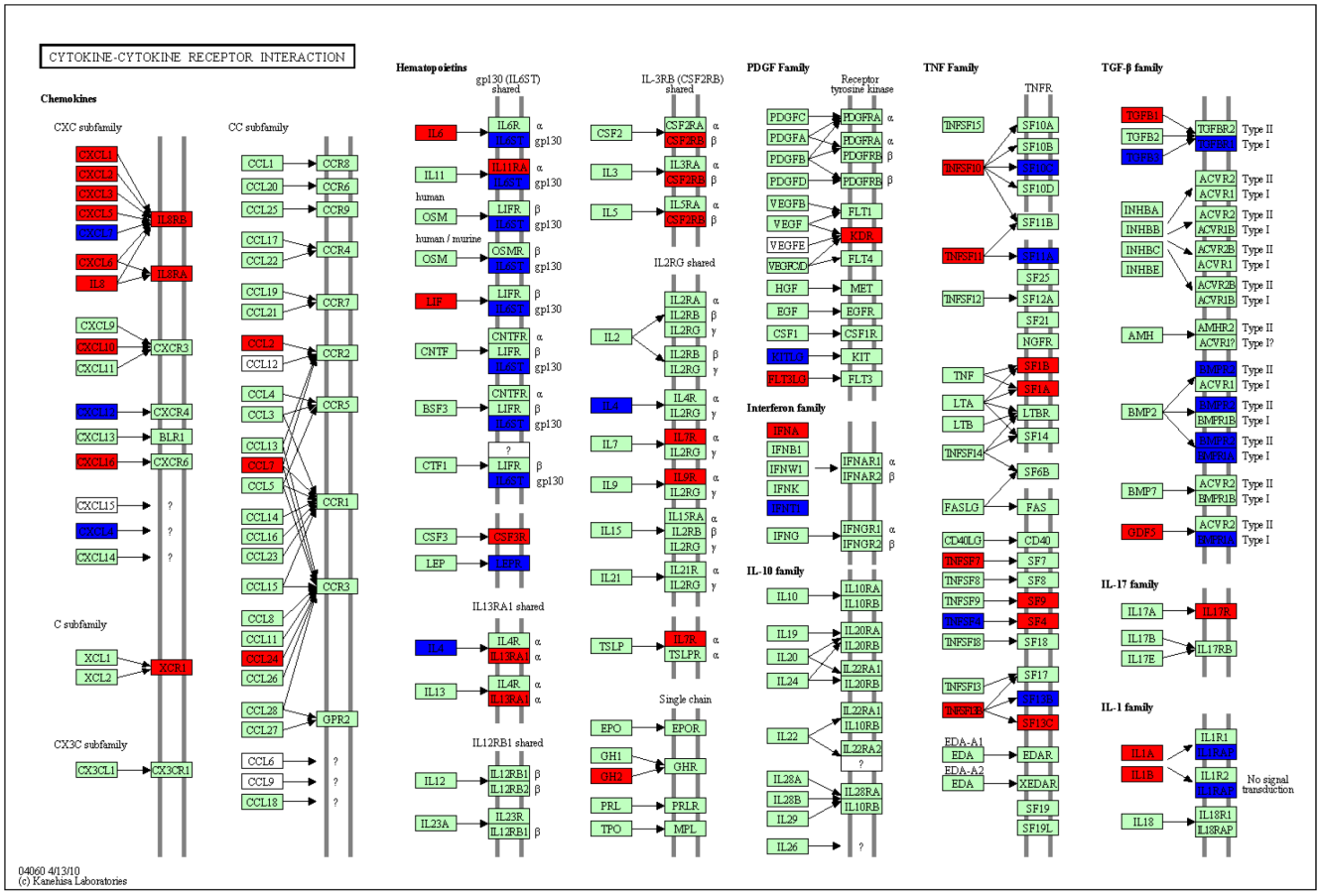

Supplementary Fig. 7. Cytokine-cytokine receptor interaction pathway map in KEGG presented with relative gene expression of 36 hr/Con.
Red: up-regulated genes, Blue: down-regulated genes, Green: unchanged genes.